NASA TECHNICAL NOTE

NASA TN D-3785

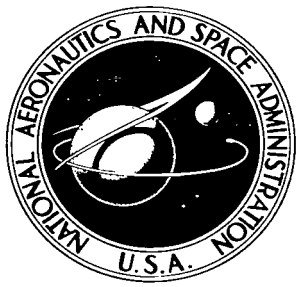

NASA TN D-3785

THERMAL CHARACTERISTICS OF A STORAGE VESSEL ON THE MOON

by James K. Harrison

George C. Marshall Space Flight Center
Huntsville, Ala.

NATIONAL AERONAUTICS AND SPACE ADMINISTRATION • WASHINGTON, D. C. • JANUARY 1967

THERMAL CHARACTERISTICS OF A STORAGE VESSEL ON THE MOON

By James K. Harrison

George C. Marshall Space Flight Center
Huntsville, Ala.

NATIONAL AERONAUTICS AND SPACE ADMINISTRATION

For sale by the Clearinghouse for Federal Scientific and Technical Information
Springfield, Virginia 22151 – Price $2.50

TABLE OF CONTENTS

	Page
SUMMARY	1
INTRODUCTION	1
ASSUMPTIONS	2
THERMAL ANALYSIS	2
VIEW FACTORS	6
Diffuse Radiation	6
Nondiffuse Radiation	10
COMPUTER PROGRAM	11
General	11
Property Data	13
Configurations	15
Time Reference	15
RESULTS	16
General	16
Temperatures	16
Thermal Conductivity	19
Shadow Cast on Moon's Surface	19
View Factors	19
Nondiffuse Radiation	21
Shape and Size of Vessel	21
Number of Isothermal Elements	22
Absorptance and Emittance	22
CONCLUSIONS	22
REFERENCES	46

LIST OF ILLUSTRATIONS

Figure — Page

1. Three Basic Shapes 23
2. Temperature - Entropy Diagram for Venting 23
3. Angle α Between Vectors $\vec{N}$ (through Center of Element) and $\vec{S}$ (to Sun) 24
4. Shadow Length for a Given Position of the Sun 24
5. Sphere (Code Number = 0) 25
6. Cylinder with Hemispherical Ends (Code Number = -1) 26
7. Cylinder with Flat Ends (Code Number = +1) 27
8. Spherical Tank Element Temperature Variations (Run 5) 28
9. Element Temperature Variations Based on a Thin Layer of Insulation (Run 10) 29
10. Energy Absorbed by Liquid Hydrogen for Runs 5 and 10 30
11. Temperature Comparison Between Run 5 (Shadow Included) and Run 11 (Shadow Excluded). Element 2, 4, 1 31
12. View Factors for Element 1, 1, 1 (Run 5) 32
13. View Factors for Element 2, 4, 1 (Run 5) 33
14. View Factors for Element 2, 4, 1 (Run 3) 34
15. View Factors for Element 1, 3, 1 (Run 3) 35
16. View Factors for Nondiffuse Radiation (Run 20) Element 1, 1, 1 36
17. View Factors for Nondiffuse Radiation (Run 20) Element 2, 4, 1 37

LIST OF ILLUSTRATIONS (Concluded)

Figure | Page

18. Temperature Comparison Between Diffuse cos ϵ (Run 11), Nondiffuse cos $^{2/3}$ ϵ (Run 25) and cos $^{1/9}$ ϵ (Run 24) Infrared Radiation. Element 1, 1, 1 38

19. Temperature Comparison Between Diffuse cos ϵ (Run 11), Nondiffuse cos $^{2/3}$ ϵ (Run 25) and cos $^{1/9}$ ϵ (Run 24) Infrared Radiation. Element 2, 4, 1 39

20. Temperature Comparison Between Diffuse (Run 11) and Nondiffuse (Run 23) Reflected Radiation. Element 1, 1, 1. 40

21. Temperature Comparison Between Diffuse (Run 11) and Nondiffuse (Run 23) Reflected Radiation. Element 2, 4, 1. 41

22. Temperature Comparison Between Diffuse (Run 11) and Nondiffuse (Run 20) for Combined Infrared and Reflected Radiation. Element 1, 1, 1 42

23. Temperature Comparison Between Diffuse (Run 5) and Nondiffuse (Run 19) Infrared Radiation. Element 2, 4, 1 43

24. Temperature Comparison Between Diffuse (Run 5) and Nondiffuse (Run 19) Infrared Radiation. Element 1, 1, 1 44

25. Temperature Comparison Between Elements of Different size but Similar Location on the Storage Vessel 45

LIST OF TABLES

Table		Page
I.	Results of Experimental Investigations of Heat Flow During Space Storage Through Penetrations	5
II.	Input Data	12
III.	Output Data	13
IV.	Multifoil Insulation Data Similar to NRC-2 Aluminized Mylar	14
V.	Multifoil Insulation Data Taken from Information on Linde Super Insulation	14
VI.	Identifying Notation and Number of Elements for One Layer of Insulation	15
VII.	Numerical Values Used in Computations	17
VIII.	Summary of Calculations	18
IX.	View Factors for Nondiffuse Infrared Radiation from Lunar Surface	20

ACKNOWLEDGEMENT

Mrs. Judy Blackwell did the scientific programming for this problem. Her steadfast interest and perseverance in the face of innumerable changes resulted in a much improved program.

THERMAL CHARACTERISTICS OF A STORAGE VESSEL ON THE MOON

SUMMARY

A theoretical analysis has been performed to study the thermal characteristics of a liquid hydrogen storage vessel on the moon. Investigations were conducted concerning the influences on temperature and propellant venting by such factors as insulation thermal conductivity, nondiffuse lunar radiation, the shadow cast by the vessel on the lunar surface, shape and size of the vessel, number of isothermal elements into which the vessel surface is divided, and the solar absorptance and infrared emittance ratio of the vessel surface.

No calculations were made to estimate the heat transfer through structural penetrations. Neither was an effort made to optimize the weight of the insulation and the evaporated propellant or to minimize the boil-off by use of techniques such as shadow shields.

The factors found to have the most influence were: thermal conductivity of insulation, size and shape of vessel, solar absorptance and infrared emittance ratio, and shadow cast by the vessel on the lunar surface.

INTRODUCTION

A computer analysis has been performed to study the thermal characteristics of objects on the lunar surface. Because of the probability of storing liquid hydrogen on the moon in the not too distant future, a vessel containing this liquid was chosen as a typical example. Investigations were conducted concerning the influences on temperature and propellant venting by such factors as insulation thermal conductivity, nondiffuse lunar radiation, the shadow cast on the moon by the vessel, shape and size of the vessel, number of isothermal elements on the vessel surface and the solar absorptance and infrared emittance ratio (α / ϵ) of the vessel surface.

No calculations were made to estimate the heat transfer through structural penetrations. The structural details of the vessel were not defined well enough to make a realistic analysis. Neither was a special effort made to optimize the weight of the insulation and the evaporated propellant or to minimize the boil-off by use of techniques such as shadow shields. The computer program can handle three vessel shapes: a sphere, a cylinder with hemispherical ends and a cylinder with flat ends. Calculations can be performed for any location of the vessel on the lunar surface.

ASSUMPTIONS

The following conditions were imposed on the analysis:

1. The moon is a flat circular area of radius $\bar{r}$.

2. The intensity equator* coincides with the selenographic equator.

3. The cryogenic liquid obeys the laws of classical thermodynamics. No reduced gravity or nonequilibrium effects are included.

4. The storage container radiates to the lunar surface and to space and receives radiation from the lunar surface and from the sun. No other sources or sinks are present.

5. The storage container is covered with a high performance, multifoil insulation located between metal surfaces. The design of the container is only crudely specified. The basic shapes are shown in Figure 1.

6. The ullage pressure at which venting begins is one atmosphere. Venting occurs at constant temperature and pressure. The initial temperature and pressure are 20.4° K and one atmosphere, respectively.

7. An initial ullage of 10 percent, by volume, was assumed.

THERMAL ANALYSIS

The temperature of objects on the moon will be nonisothermal, especially large surfaces which are only partly illuminated. To minimize this, the insulation on the storage vessel has been divided into elements. By increasing the number of elements each one approaches an isothermal condition at any instant of time because its size diminishes. This increases the accuracy of the results as well as the complexity of the problem.

The temperature of an element at any time is given by

* Line containing subsolar point and subearth point.

$$C_i \frac{dT_i}{dt} = \sum_{j=1}^{M} C_{ij} (T_j - T_i) + D_1 R_1 f S + D_1 R_2 S + D_1 R_3 (T_s - T_i)$$

$$+ R_4 (T_m^4 - T_i^4) - R_5 T_i^4, \quad (i = 1, 2, \ldots, N) \qquad (1)$$

where

C_i = total heat capacity of element $i (= \rho_i v_i c_i)$

T_i = temperature of element i

t = time

C_{ij} = conduction coupling term between elements i and j $\left(\frac{k_{ij} A_{ij}}{\ell_{ij}}\right)$

D_1 = a constant set equal to 0 (lunar night) or 1 (lunar day)

R = radiation coupling terms. They are, in the order listed in the equation, composed of the following quantities:

$(\bar{A}_t F_r \alpha)$, $(\bar{A}_t F \alpha)$, $(\bar{A}_t F_{s,\alpha} \epsilon \epsilon_m \sigma)$, $(\bar{A}_t F'_m \epsilon \epsilon_m \sigma)$

and $[A_t (1 - F_m) \epsilon \sigma]$

$A_t, \bar{A}_t$ = total and projected surface area, respectively, of element i

$F_r, F, F_{s,\alpha}, F'_m, F_m$ = view factors with respect to reflected sunlight, direct insolation, shadow, and moon (with and without shadow), respectively

α, ϵ = total solar absorptance and infrared emittance of vessel surface

σ = Stefan-Boltzmann's constant

S = solar constant

f = moon's total local albedo

ϵ_m = moon's infrared emittance

The terms on the right-hand side of the equation represent, in the order listed, heat exchange with the following sources and sinks: adjacent elements, lunar reflected sunlight, insolation, shaded region of moon's surface, unshaded region of moon's surface, and space. Equation (1) is required for each element in order to compute the temperature as a function of time and is solved numerically.

Knowing each temperature, the heat transfer to the liquid per unit time is calculated by

$$\dot{q} = \sum_{i}^{n} C_{i-\ell} (T_i - T_\ell) \tag{2}$$

where

n = number of elements adjacent to liquid

$C_{i-\ell}$ = conduction coupling terms from element i to liquid $\left(= \frac{k_{i-\ell} A_{i-\ell}}{\ell_{i-\ell}} \right)$

T_ℓ = temperature of cryogenic liquid

and the sum total of the energy transferred over any time increment is

$$q = \sum_{1}^{m} \dot{q} \, \Delta t \tag{3}$$

where

Δt = a single time increment

m = number of time increments counting from beginning of storage period

The heat transfer to the liquid because of the insulation temperature is, unfortunately, not the total. Structural penetrations are always present and cause a degradation in the effectiveness of the insulation. This has been studied experimentally (Table I). In this analysis attempts to calculate the heat transfer from structural penetrations were abandoned, being too unrealistic with such an ill-defined design. Rather, this heat was accounted for by assuming that a given percent of the total heat absorbed by the liquid resulted from structural penetrations. This was made a parameter, and three values were used: 0, 20 and 50 percent. Therefore, the total heat absorbed by the liquid is

$$\dot{Q} = \dot{q} + \left(\frac{x}{1 - x} \right) \dot{q} = \dot{q} \left(\frac{1}{1 - x} \right) \tag{4}$$

where

x = fraction of heat absorbed resulting from penetrations

TABLE I

RESULTS OF EXPERIMENTAL INVESTIGATIONS OF HEAT FLOW DURING SPACE STORAGE THROUGH PENETRATIONS

Reference	Insulation	Percent of Total Energy Transferred Through Structural Penetrations	Remarks
General Electric Company [1]	Linde SI-62 & NRC-2	28-85	3 spherical vessels (2, 4, & 8 ft. in diameter) 1 cylindrical vessel (3 ft. in diameter by 6 ft. in length)
Boeing Company [2]	Linde	24	Ellipsoidal 8 ft. diameter vessel

and the sum total, since the beginning of the storage period, is

$$Q = \sum \dot{Q} \Delta t. \tag{5}$$

The evaporation rate $\dot{m}$ at any time is

$$\dot{m} = \dot{Q} / L_v \tag{6}$$

where

L_v = latent heat of evaporation

and the total amount evaporated, m, at any time, is

$$m = \sum Q / L_v \tag{7}$$

If no venting occurs, the temperature of the liquid will rise (Fig. 2). During such a process the temperature at any time is given by

$$T_f = T_i + \frac{\Delta t}{C} q \tag{8}$$

where

T_i, T_f = initial and final temperature, respectively, during time increment Δt

C = heat capacity of liquid [$c\ (m_0 - m)$]

c = specific heat capacity of liquid

m_0 = initial liquid mass

m = liquid mass evaporated as given by eq. (7)

If venting occurs, the temperature will remain constant sc long as the ullage pressure is constant (Fig. 2). The vent rate $\dot{m}^*$ at any time is

$$\dot{m}^* = \left(1 - \frac{\rho_g}{\rho_\ell}\right) \dot{m} \tag{9}$$

and the total amount vented m^* up to time t is

$$m^* = \left(1 - \frac{\rho_g}{\rho_\ell}\right) m \tag{10}$$

where

ρ_g, ρ_ℓ = density of cryogenic vapor and liquid, respectively

$\dot{m}$ = evaporation rate

m = total evaporated liquid

VIEW FACTORS

Diffuse Radiation

The radiation exchange terms in eq. (1) require view factors for each surface element. The view factor for the direct impinging sunlight (Fig. 3) is

$$F = \cos \alpha \tag{11}$$

where

α is angle between vectors $\vec{N}$ and $\vec{S}$ (Fig. 3).

Four view factors for diffuse lunar radiation are necessary: (1) reflected sunlight, F_r, (2) shadow emission $F_{s,\alpha}$ (when such exists), (3) emission from unshaded part of moon, F_m', or (4) emission from total moon when no shadow exists, F_m. These view factors are computed from the same expression although modifications* are necessary, i.e., $F_{s,\alpha}$ will be with respect to a much smaller area than F_m. The basic expression [3] is

$$F = \frac{\cos\gamma}{\pi}\left[\frac{\pi R^2}{2(R^2+1)} - \frac{R^2 \sin^{-1}\left(-\frac{\cot\gamma}{R}\right)}{R^2+1} + \frac{\cot\gamma \cos^{-1}\left(\frac{\cot^2\gamma+1}{1+R^2}\right)^{\frac{1}{2}}}{(\cot^2\gamma+1)^{\frac{1}{2}}}\right]$$

$$+ \frac{\sin\gamma}{\pi}\left[-\frac{(R^2-\cot^2\gamma)^{\frac{1}{2}}}{R^2+1} + \frac{\cos^{-1}\left(\frac{\cot^2\gamma+1}{1+R^2}\right)^{\frac{1}{2}}}{(\cot^2\gamma+1)^{\frac{1}{2}}}\right]^{**} \qquad (12)$$

where

γ = angle between normals to vessel element and lunar surface

R = ratio of radius of circular area representing the moon's surface to height of vessel element above surface of moon $\left(=\frac{\bar{r}}{\bar{h}}\right)$

This view factor applies for radiation exchange between a differential element and a finite circular area of radius $\bar{r}$. The differential element is centered and above the circular area by a distance $\bar{h}$. The elements on the vessel, because

---

* Except for F_r which will be equal to F_m' for the diffuse case.

** For cases where $R = \infty$ this becomes, by L'Hospital rule, $\frac{1}{2}(1+\cos\gamma)$ or $\cos^2\left(\frac{\gamma}{2}\right)$: if $\cot\gamma > R$, set $\cot\gamma = R$. For cases where $\gamma = 0$,

$$F = \frac{\bar{r}^2}{\bar{r}^2 + \bar{h}^2}.$$

they are very small compared to the circular area, are taken as the differential area.

To get the view factor for the shaded part of the moon, the size of the shadow must be estimated. It will vary from a circle (with a diameter equal to the diameter of the storage vessel), when the sun is directly overhead, to a rectangle of great length, when the sun is just rising or setting. This length (Fig. 4) is given by

$$\ell = \frac{h + 2r}{\tan \nu} \quad . \tag{13}$$

The angle ν is given by

$$\nu = \sin^{-1} \left(\sin \bar{\xi} \sqrt{1 - \sin^2 \lambda} \right) \tag{14}$$

where

$\bar{\xi}$ = time angle of sun (equal to 0° when sun first rises above horizon, to 90° when sun is directly overhead, etc.)

λ = latitude location of vessel

If the vessel is a cylinder with hemispherical ends, the height $\bar{h}$ of an element (above the moon's surface) located on the lower hemisphere, middle cylinder, and upper hemisphere are given by

$$\bar{h} = d + r + r\vec{N}_z \tag{15a}$$

$$\bar{h} = d + r + \tfrac{1}{2}h \tag{15b}$$

$$\bar{h} = d + r + h + r\vec{N}_z \tag{15c}$$

respectively, where

d = vertical distance from lowest point of vessel to lunar surface (= 1 for all calculations)

r = radius of vessel

h = height of middle

$\vec{N}_z$ = vertical component of $\vec{N}$ ($\vec{N}$ is the vector through center of element from center of vessel)

When the vessel is a sphere, eq. (15b) is not involved and when the vessel is flat ended, eqs. (15a) and (15c) are not involved. The ratio R_s, required for calculating with eq. (12) the shadow view factor, F_s, is

$$R_s = \frac{\ell}{2\bar{h}} \tag{16}$$

Further modifications are required since the view factor calculated using eq. (12) is for a circular area (which the shadow is not, except when the sun is directly overhead). An approximation to the correct value can be made by

$$F_s' = \frac{A_e}{A_0} F_s \tag{17}$$

where

A_0 = area of shadow if circular with radius $\frac{\ell}{2}$

A_e = area of shadow if rectangular with length ℓ

Elements on the vessel that are fully facing the shadow will be more strongly influenced than others. Those that are on the side away from the shadow, of course, will not be influenced at all. This is included in the view factor calculations for a given element, by finding the cosine of the angle between the $-\vec{S}$ and $\vec{N}$ vectors and multiplying by F_s' or

$$F_{s,\alpha} = \cos \alpha' F_s' \tag{18}$$

where

α' = angle between $-\vec{S}$ and $\vec{N}$

$F_s^{\bullet}$ = view factor calculated using R_s

The view factor for the unshaded part of the moon is found from

$$F_m' = F_m - D_1 F_{s,\alpha} \tag{19}$$

where

D_1 = constant having value of 1 during lunar day and 0 during lunar night

Nondiffuse Radiation

The nondiffuse radiation is included in the calculations by modifying the view factors for infrared radiation and solar reflected radiation. Previously, these were computed from the same expression [eq. (12)].

For diffuse radiation, the view factor is given by

$$F_{1-2} = \int_{A_2}\int_{A_1} \frac{\cos\ \epsilon \cos\ \Theta\ dA_1 dA_2}{\pi\ r^2} \tag{20}$$

If the radiation is nondiffuse, an expression must be found which characterizes the radiation, as does Lambert's equation for diffuse radiation. For the infrared radiation, the expression of Pettit and Nicholson [4] is used:

$$I = I_0 \cos^{2/3} \epsilon \tag{21}$$

and for the reflected sunlight, the expression of Hapke [5] is used (after being normalized to equal I_0 at its maximum value):

$$I = I_0 \left(\frac{\cos\ i}{\cos\ i + \cos \epsilon}\right) \left(\frac{\sin\alpha + (\pi - \alpha)\cos\ \alpha}{\pi}\right) \left(B\ (\alpha, g)\right) \tag{22}$$

where

I = radiant energy per unit time per unit area per unit solid angle

I_0 = maximum value of I

ϵ = angle between normal to lunar surface and emitted or reflected beam of radiation

i = angle between normal to lunar surface and incident beam of solar energy

α = phase angle, angle between emitted or reflected beam and incident beam

$$B(\alpha, g) = \left\{ 2 - \frac{\tan\ \alpha}{2g}\ (1-e^{-g/\tan\ \alpha})(3-e^{-g/\tan\ \alpha}) \right\},\ \alpha < \frac{\pi}{2}$$

$$B(\alpha, g) = 1,\ \alpha \geq \frac{\pi}{2}$$

$g = \frac{2r}{\lambda}$ (r is the radius of a tube, λ is the mean free path of light ray through lunar surface, and g is assumed to be 0.8.)

Because the view factor is between a differential element A_2 and a finite area A_1, the integration over A_2 is eliminated. The view factor expression is now written in a general way as

$$F_{1-2} = \int_{A_1} \frac{\Psi(\epsilon, \varphi) \cos\Theta \, dA_1}{k\pi r^2} \tag{23}$$

and the function $\Psi(\epsilon, \varphi)$ is given by the expressions which follow. For diffuse radiation, $\cos\epsilon$; for nondiffuse infrared radiation, $\cos^{2/3}\epsilon$; and for nondiffuse reflected radiation, $\left(\frac{\cos i}{\cos i + \cos \epsilon}\right)\left(\frac{\sin\alpha + (\pi - \alpha)\cos\alpha}{\pi}\right)\left(B(\alpha, g)\right)$.

The k in the denominator is a normalizing factor equal to unity for the diffuse case and other than unity for the nondiffuse case. The view factors are calculated by numerical methods and substituted into the proper terms in eq. (1). The results are presented later.

COMPUTER PROGRAM

General

A computer program has been prepared to predict the thermal behavior of the vessel and its contents. The program is a combination of several smaller programs. The cross-sectional area and lengths for the conduction terms are calculated in a separate subroutine [6]. The view factors for nondiffuse radiation are computed in a separate program and read into the main program as input data. The view factors for diffuse radiation are calculated within the main program. The moon's temperature is computed from a Fourier series [7] which is a subroutine. * The shadow cast on the lunar surface was assumed to have a uniform temperature of 109 °K. Theoretical calculations have shown that no appreciable gradient exists in the region about the edge of the shadow and that a single constant temperature can be assigned to the shadow area [9]. The Heun method [10] with an automatic time step criteria [11] is used to solve the differential equations. Computer time for a run over one lunar cycle varies (16 to 170 minutes), but 80 percent of the runs took 20 minutes or less. A report is being prepared which gives the details of the program, i.e., listing, flow chart, deck setup instructions, etc. [12].

* The Fourier series was fitted to Sinton's data [8]. Variations in temperature with latitude are taken into account by multiplying by cos λ where λ is the latitude.

The computer program parameters are listed in Tables II and III.

TABLE II

INPUT DATA

Parameter	Notation
Identification of the number of elements in each layer of insulation (Table VI)	N
Insulation thickness	L
Number of layers into which insulation is divided	K
Radius of vessel	r
Height of cylindrical middle, when present	h
Designates shape; sphere, cylinder with flat ends, cylinder with hemispherical ends, respectively	0, 1, -1
Latitude location of vessel	λ
Solar absorptance of vessel surface	α
Infrared emittance of vessel surface	ϵ
Insulation thermal conductivity normal to insulation	k_n*
Insulation thermal conductivity parallel to insulation	k_ℓ*
Insulation specific heat	c*
Insulation density	ρ
Cryogenic liquid specific heat	c_ℓ*
Cryogenic liquid density	ρ_ℓ*
Vessel ullage gas density	ρ_g*
Albedo of moon	f
Vent valve opening pressure	None
Metric (MKS) or English system of units	None

* These property data are temperature dependent. They are either read-in from a table (i.e., Table IV) or expressions are used to give the values as a function of temperature.

TABLE III

OUTPUT DATA

Parameter	Notation
Temperature of each element, of cryogenic liquid, and of moon	T
Cross-sectional area of elements, lengths between adjacent elements, volume of elements and other geometry data [6]	A, ℓ, V
Insulation weight	None
View factors	F
Heat transferred to liquid through insulation and through penetrations (supports)	$\dot{q}$
Evaporation rate	$\dot{m}$
Vent rate	$\dot{m}$*
Percent vented	None
Initial liquid mass	m_0
Liquid mass evaporated	m

Property Data

The temperatures at the end of each time step were used as a basis for selecting the thermal properties for the succeeding computation. The thermal property data used for the multifoil insulation are presented in Tables IV and V. Table IV gives data that approximately coincide with the NRC-2 aluminized Mylar insulation. For NRC-2 insufficient data were available over the temperature range of interest, therefore, assumptions* were necessary. The values that were taken from the literature (and they comprise only a few) are noted. Table V gives data taken from information supplied by the Linde Company on their super-insulation. No assumptions are involved here.

* These assumptions involved extrapolations, interpolations, and assumptions about the slope of the curves.

The data used for the liquid hydrogen were taken from reference 13. All the data are for equilibrium liquid hydrogen.

TABLE IV

MULTIFOIL INSULATION DATA SIMILAR TO NRC-2 ALUMINIZED MYLAR

T (°K)	c (J/kg -°K)	k_n (W/m- °K)	k_ℓ (W/m -°K)	ρ [14] (kg/ m^3)
20	0.14×10^3	3.95×10^{-5}	0.082	41.648
100	0.70×10^3	1.37×10^{-4}	0.138	41.648
200	1.37×10^3	4.00×10^{-4} [14]	0.148 [16]	41.648
300	2.05×10^3 [15]	9.70×10^{-4}	0.149	41.648
400	2.70×10^3	2.10×10^{-3}	0.150	41.648
500	3.40×10^3	4.35×10^{-3}	0.150	41.648
600	4.00×10^3	9.00×10^{-3}	0.150	41.648

TABLE V

MULTIFOIL INSULATION DATA TAKEN FROM INFORMATION ON LINDE SUPER INSULATION *

T (°K)	c (J/kg - ° K)	k_n (W/m - °K)	ρ (kg/m^3)
16.7	0.01255×10^3	0.2767×10^{-5}	112.1
111.1	0.3766×10^3	0.1280×10^{-4}	112.1
222.2	0.7113×10^3	0.4324×10^{-4}	112.1
333.3	0.9623×10^3	1.159×10^{-4}	112.1
444.4	1.172×10^3	2.421×10^{-4}	112.1
500.0	1.297×10^3	3.459×10^{-4}	112.1
833.3	1.883×10^3	1.557×10^{-3}	112.1

* Data obtained from the Linde Company.

Configurations

The computer is programmed to perform calculations for three vessel shapes: a sphere, a cylinder with hemispherical ends, and a cylinder with flat ends. The insulation for each shape can be partitioned three different ways. Each way provides a different number of elements. The insulation can be further partitioned into layers. Three was the normal number of layers used for almost all calculations. This information is summarized in Table VI and is depicted in Figures 5 through 7. The information in Table VI is for one insulation layer; for three layers the number of elements will be tripled.

TABLE VI

IDENTIFYING NOTATION AND NUMBER OF ELEMENTS FOR ONE LAYER OF INSULATION

N	Sphere (Code = 0)	Cylinder with Hemispherical Ends (Code = -1)	N	Cylinder with Flat Ends (Code = +1)
8	8	12	8	12
32	32	40	16	24
72	72	84	24	36

Time Reference

In this analysis, time (in hours) is given relative to the lunar midnight. The mean synodic period (time required for subsolar point to travel full 360° around the lunar surface) is 29.530589 earth days and is taken as one full lunar cycle. Calculations requiring time dependent angular measurements are relative to the time angle ξ defined by the following expression

$$\xi = \left(\frac{360}{(29.530589)(24)} \right) t$$

$$\xi = 0.507948t \qquad (24)$$

where t is in hours.

RESULTS

General

Table VII shows the numerical values used to make the calculations. The values apply to most, though not all, runs (the exceptions are noted). Run 5 is typical of the runs for which the values apply. Table VIII summarizes the computer results. Table VIII (reading from left to right) presents the following: the run number, identification for the number of elements in each layer of insulation (Table VI), the code that designates the tank shape (Table VI), the radius of the vessel, the lunar latitude location of the vessel, the percent of the liquid vented for an idealized case (no heat enters through penetrations),* the ratio of percent vented to percent vented for Run 5 (used as a standard of comparison), and pertinent remarks that distinguish one run from the other. The initial mass of liquid hydrogen was obtained by using tank dimensions which correspond roughly with those of payloads compatible with the Lunar Module. This approach was taken by A. D. Little [9] and seems reasonable. However, one other size has been investigated (Table VIII, Run 2).

Temperatures

Figure 8 shows the temperatures for Run 5 for the elements indicated. The location of the elements are shown in Figure 5a, pertinent information about the run is given in Table VIII.** Elements 5 and 6 are in the third layer. The temperature characteristics are reasonable (and typical of the other runs) when the location of each element is considered. Figure 9 shows the temperature for a case where calculations were based on a very thin layer of insulation. This was done to allow the temperatures to achieve steady state. These temperatures were used, with the regular insulation thickness (10.16 cm; 4 inches), to calculate the venting. Although the temperature difference between Run 5 (outside layer) and Run 10 is negligible, some difference is present in the heat transfer (Fig. 10). The shift in the curves is caused by the differences in insulation heat capacity (much higher for Run 5). If the curves peaked at the

* An estimate of the venting for cases where structural penetrations are present may be made by straight multiplication of the values in the table. For example, if 50 percent of the total flux is assumed to be due to penetrations, the table value for percent vented would be doubled.

** Information about all figures can be obtained by referring to Table VIII.

TABLE VII

NUMERICAL VALUES USED IN COMPUTATIONS

	Insulation weight [1]	223.3 kg (492.3 lbs)
L	Insulation thickness[2]	10.16 cm(4.0 inches)
m_0	Initial propellant[3] weight	2187.9 kg (4823.4 lbs)
r	Vessel radius[4]	2.1 m (6.88 ft)
	Vessel volume[5]	38.79 m^3 (1369.86 ft^3)
ϵ_m	Moon's infrared emittance	1.00
f	Albedo of moon	0.07
S	Solar constant	1395 W/m^2
ϵ	Vessel infrared[6] emittance	0.90
α	Vessel solar absorptance[6]	0.20
T	Initial liquid hydrogen temperature	20.4°K
p	Initial ullage pressure	1 atm
	Initial ullage	10 % by volume
$\bar{r}$	Radius of lunar surface	520 m (1706 ft)
$\bar{A}_t$	Projected surface area[7] of an element on vessel	4.41 m^2 (47.47 ft^2)
A_t	Surface area of an element[7] on vessel	6.93 m^2 (74.59 ft^2)
σ	Stefan-Boltzmann's constant	5.673×10^{-8} $W/m^2 - °K^4$

[1]All weights are with respect to earth gravity. Run 2, 53.13 kg (117.1 lbs); Run 21, 601.1 kg (1325.2 lbs); Run 10, 4.61 kg (10.16 lbs); Run 3, 269.8 kg (594.8 lbs); Run 4, 233.7 kg (515.2 lbs).

[2]Run 22, 3.534 cm (1.39 in); Run 10, 0.2 cm (0.07874 in)

[3]Run 2, 273.5 kg (603.0 lbs)

[4]Run 2, 1.05 m (3.44 ft); Run 4, 1.68 m (5.51 ft)

[5]Run 2, 4.85 m^3 (171.24 ft^3)

[6]Run 14, $\alpha = \epsilon = 1.0$

[7]Does not apply to Runs 2, 3, 4, and 7. Run 7, $\bar{A}_t = 0.74$ m^2 (0.80 ft^2), $A_t = 0.77$ m^2 (0.83 ft^2)

TABLE VIII

SUMMARY OF CALCULATIONS

Run No.	N	Shape Code	r	λ	Percent Vented (1 lunation)	Percent Vented Ratio	Remarks (Deviations from Run 5)
1	8	0	2.1	30	5.53	0.96	
2	8	0	1.05	30	11.39	2.06*	
3	8	+1	2.1	30	7.35	1.33*	h = 2.8
4	8	-1	1.68	30	6.17	1.12*	h = 2.13507
5	8	0	2.1	0	5.79	1.00	
7	72	0	2.1	30	6.20	1.12*	216 elements
8	8	0	2.1	0	22.09	3.82	Property data constant at 300 °K
9	8	0	2.1	0	5.81	1.00	$k_\ell = 0$
10	8	0	2.1	0	4.55	0.79	Thin insulation, $k_\ell = 0$
11	8	0	2.1	0	6.64	1.15	Shadow view factor is zero
14	8	0	2.1	0	8.51	1.47	$\alpha = \epsilon = 1$
15	8	0	2.1	0	9.46	1.63	Property data constant at 200 °K
19	8	0	2.1	0	5.89	1.02	$\cos^{2/3}\epsilon$ function
20	8	0	2.1	0	6.58	0.99**	Hapke function, $\cos^{2/3}\epsilon$ function, shadow view factor is zero
21	8	0	2.1	0	0.37	0.06	Linde insulation with thickness 10.16 cm
22	8	0	2.1	0	1.45	0.25	Linde insulation with thickness 3.534 cm
23	8	0	2.1	0	6.64	1.00**	Hapke function, shadow view factor is zero
24	8	0	2.1	0	6.53	0.98**	$\cos^{1/9}\epsilon$ function, shadow view factor is zero
25	8	0	2.1	0	6.58	0.99**	$\cos^{2/3}\epsilon$ function, shadow view factor is zero

* Compared with Run 1

** Compared with Run 11

same thermal energy value, the sums, if taken over a lunation, would be about the same. For this reason some investigators [9, 17] have used the steady state method to obtain satisfactory answers for this type of problem. In this investigation the thermal energy absorbed by the liquid hydrogen was generally higher for Run 5 than for Run 10 (Fig. 10). This is attributed to three factors: the insulation thickness, which was less for Run 5 since the overall insulation thickness is divided into 3 layers (the flux is computed using the thickness of the innermost layer) ; the temperature difference, which is less for Run 5 since the temperature of the innermost layer is used; the thermal conductivity of the insulation, which is lower for Run 5 since the temperature is lower and k_n, being temperature-dependent, decreases. The first factor increases the flux and the last two cause a decrease. The net result during most of the lunar cycle (the lunar morning excepted) is a greater thermal energy transfer for Run 5.

Thermal Conductivity

The percent vented ratio (Table VIII) clearly demonstrates the influence of a number of factors on the calculated results. The factor exerting the greatest influence is the thermal conductivity and is aptly demonstrated by a comparison of Runs 21 and 5. The insulation data shown in Table V were used in Run 21; the data in Table IV were used in Run 5. The values of k_n for Run 21 are roughly an order of magnitude smaller than for Run 5. The insulation weight increases by about a factor of 3 (Table VII). Run 22 was made keeping the insulation weight equal to that of Run 5(varying the thickness) and the results still indicate the overriding influence of k_n. Run 9 shows the negligible influence on the calculated results when the thermal conductivity in the lateral direction (k_ℓ) is zero.

Thermal properties, if assumed to be temperature independent, can lead to significant errors. This is shown by Runs 8 and 15 in Table VIII.

Shadow Cast on Moon's Surface

The effect of the shadow is not negligible. Disregarding the shadow (Run 11) gives a 15 percent increase in the percent vented over the value in Run 5 where it is included. The appreciable temperature difference between Run 5 and Run 11 is further evidence of its significance (Fig. 11).

View Factors

The view factor calculations for diffuse radiation are presented in Figures 12 through 15. Equation (12) was used to compute the view factors for infrared

and reflected radiation from the lunar surface. In Figure 12 the shadow view factor is hardly noticeable, having a maximum at 0.73 lunation (lunar noon occurs at 0.50 lunation). The location of this element (Fig. 5a) readily explains why. Figure 13 gives the same information for another element.

Figures 14 and 15 give the view factors for elements located on a cylindrical vessel with flat ends located at a latitude 30 degrees above the lunar equator (previously the vessel was a sphere located on the equator). In Figure 14 the element is facing the surface and in Figure 15 the element is vertical to the surface.

The view factor calculations for nondiffuse radiation are presented in Figures 16 and 17. For comparison, the same elements used in Figures 12 and 13 were plotted. Equation (23) was used to compute the view factors for infrared and reflected radiation from the lunar surface using the $\cos^{2/3}\epsilon$ and Hapke expressions, respectively. The shadow view factor was excluded from these calculations so the effect of reflected radiation could be determined when at its maximum (the shadow will attenuate radiation that has a large backscatter component). Figures 16 and 17 show that the view factors for reflected sunlight are very strongly dependent on the position of the sun (sunset occurs at 0.75 lunation). The view factors for infrared radiation are only slightly different from the diffuse case, and because of this, $\cos^{1/9}\epsilon$ was arbitrarily picked for comparative purposes to make additional calculations. The results for all three cases ($\cos\epsilon$, $\cos^{2/3}\epsilon$, and $\cos^{1/9}\epsilon$) are given in Table IX. The elements are located on a vessel as in Run 5.

TABLE IX

VIEW FACTORS FOR NONDIFFUSE
INFRARED RADIATION FROM LUNAR SURFACE

Element	$\cos\epsilon$	$\cos^{2/3}\epsilon$	$\cos^{1/9}\epsilon$
1, 1, 1	0.18	0.21	0.27
2, 4, 1	0.82	0.79	0.74

Notice in Table IX that for element 1, 1, 1 (upper part of vessel) the values increase from case to case, while for element 2, 4, 1 (lower part of vessel) the values decrease. Also the sum of the two elements in each case is

approximately unity. This is logical because the total radiation striking the vessel does not change (as long as the temperature of the lunar surface at the location of the vessel is constant), only the distribution of the radiation.

Nondiffuse Radiation

The influence of nondiffuse radiation from the lunar surface is included in the calculations, through the nondiffuse view factors. This effect on the temperature of the vessel elements, though small, is present (Figs. 18 and 19). Run 11 is diffuse infrared radiation given by Lambert's cos ϵ expression and Run 25 is nondiffuse infrared radiation given by Pettit and Nicholson's $\cos^{2/3} \epsilon$ expression.

Notice that the temperature for element 4 is lower in Run 25 than in 11 (Fig. 19). The reverse is true for element 1 (Fig. 18). This follows from the view factors in Table IX. Because $\cos^{2/3} \epsilon$ is such a slight departure from the diffuse case, as evidenced by the results, Run 24 was made using $\cos^{1/9} \epsilon$. This expression was arbitrarily picked for comparative purposes and has no theoretical or experimental basis.

The reflected radiation in Runs 11 and 25 was assumed to be diffuse. Hapke's expression [eq. (22)] was used for nondiffuse reflected sunlight. Although the view factors are strongly affected, the temperatures are not because of the low albedo (0.07) of the moon. This is shown in Figures 20 and 21. In Run 20 the $\cos^{2/3} \epsilon$ and Hapke's expression have been combined. Runs 20 and 11 are compared in Figure 22.

Shadow effects were not included in Runs 11, 20, 23, 24, and 25. Runs 5 and 19 contain shadow effects. Figure 23 shows that for an element facing the lunar surface the nondiffuse effect is washed-out by the shadow (except during the lunar morning). This is not so for elements facing away from the lunar surface as shown in Figure 24.

Table VIII shows that there is no influence of nondiffuse radiation on the venting. This is because the vessel receives the same total amount of energy, since it receives radiation from all directions, regardless of the spatial distribution of the radiation from the lunar surface.

Shape and Size of Vessel

Venting is influenced by the shape of the vessel as shown by Runs 1, 3, and 4 (Table VIII). All vessels have the same volume. Venting is also a strong function of size, increasing as the vessel becomes smaller (Run 2).

Number of Isothermal Elements

The accuracy of the calculations can be increased at the expense of overall complexity by dividing the insulation into a greater number of elements. This has been done in Run 7. The insulation is divided into 216 elements (most calculations are for 24 elements) and the 12 percent difference between Runs 1 and 7 represents the accuracy sacrificed when the more simple case (Run 1) is used. Of interest in these two cases is a temperature comparison (Fig. 25) for elements of similar location (Figs. 5a and 5c) but different size.

Absorptance and Emittance

The α/ϵ values of the outer surface have a profound effect on the venting and in this analysis are assumed to provide, along with the insulation, the only means of thermal control. The accumulation of materials from the moon's surface onto the vessel surface could alter the α / ϵ ratio. For this reason, Run 14 was made where $\alpha = \epsilon = 1$ was used. The results are given in Table VIII.

CONCLUSIONS

The following factors were found to have a significant influence on the thermal characteristics of a storage vessel in a lunar simulated environment: thermal conductivity normal to insulation, constant thermal properties, size and shape of the storage vessel, α/ϵ ratio, and the shadow cast by the vessel.

Nondiffuse infrared radiation (on temperature only), the number of isothermal elements on the vessel surface, and steady-state temperatures (on venting only), were found to have slight, though not necessarily negligible influence on the vessel.

There was no appreciable influence resulting from the lateral thermal conductivity of insulation and reflected sunlight (neither diffuse nor nondiffuse).

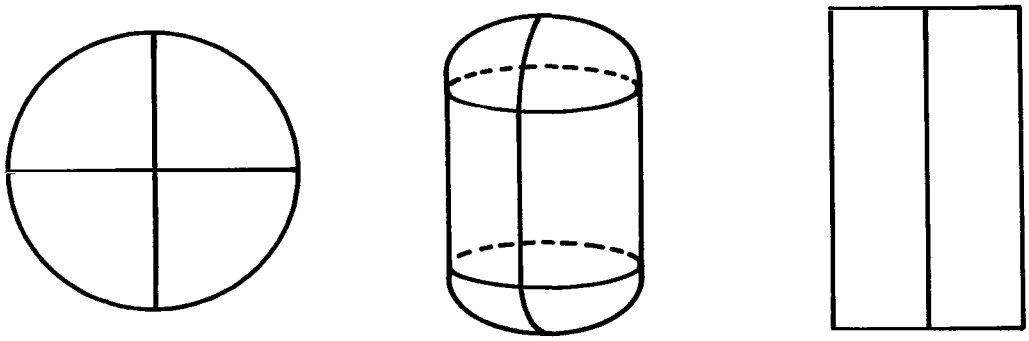

FIGURE 1. THREE BASIC SHAPES

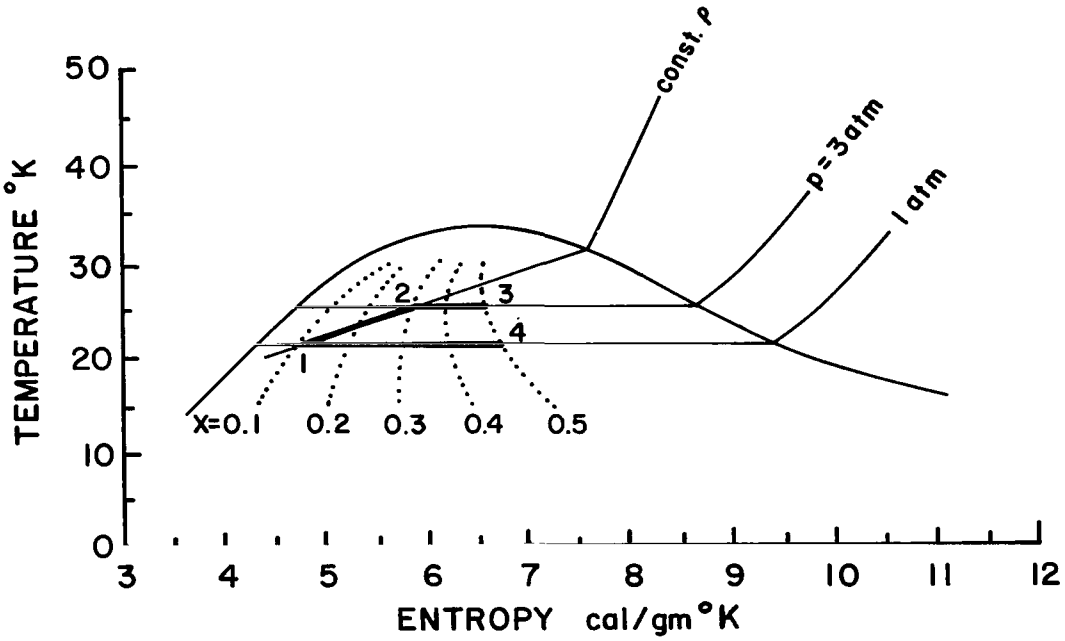

1. No venting (1-2)
2. Venting begins and pressure and temperature remains constant (2-3)
3. Venting occurs during entire storage period (1-4)

FIGURE 2. TEMPERATURE - ENTROPY DIAGRAM FOR VENTING

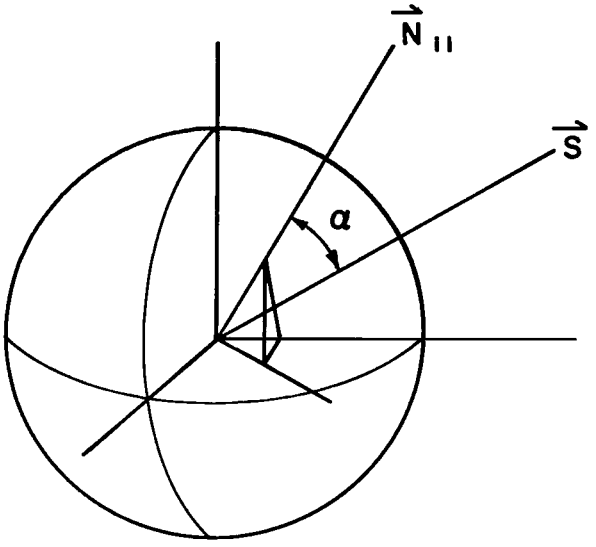

FIGURE 3. ANGLE α BETWEEN VECTORS $\vec{N}$ (THROUGH CENTER OF ELEMENT) AND $\vec{S}$ (TO SUN)

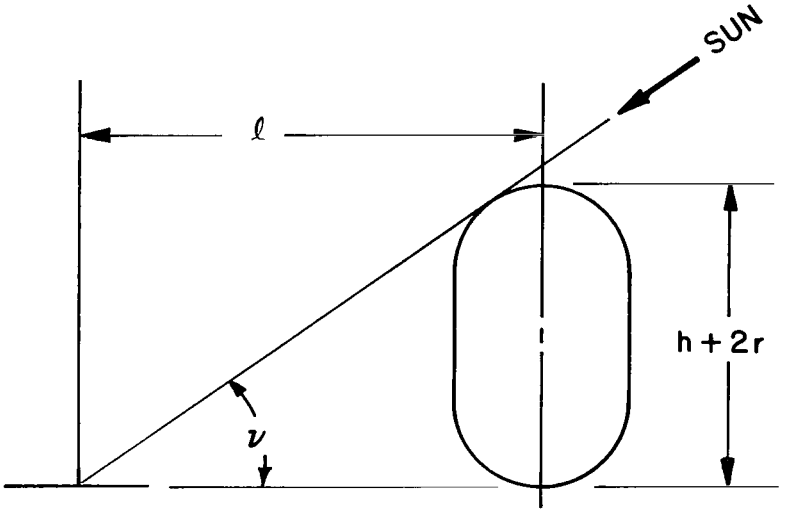

FIGURE 4. SHADOW LENGTH FOR A GIVEN POSITION OF THE SUN

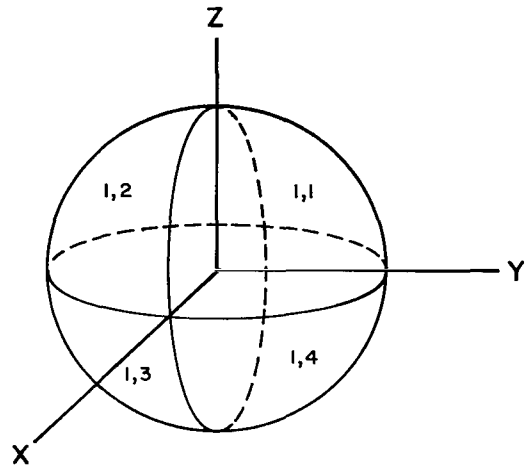

(a) N = 8 - NUMBER OF ELEMENTS = 8

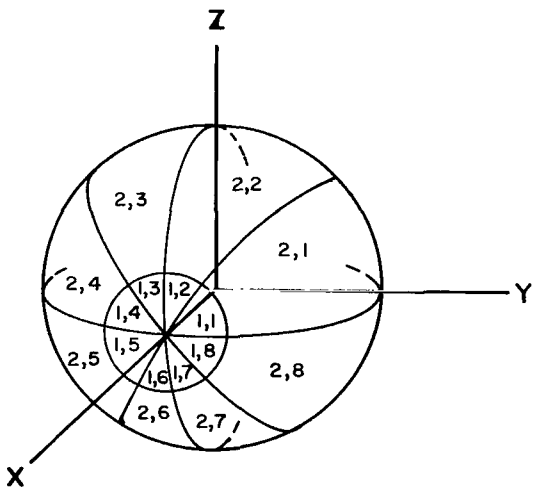

(b) N = 32 - NUMBER OF ELEMENTS = 32

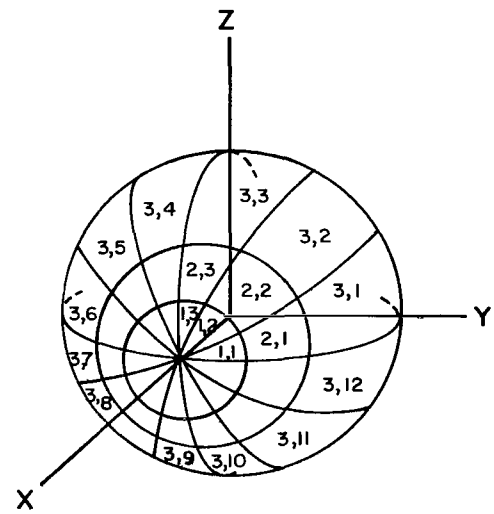

(c) N = 72 - NUMBER OF ELEMENTS = 72

FIGURE 5. SPHERE (CODE NUMBER = 0)

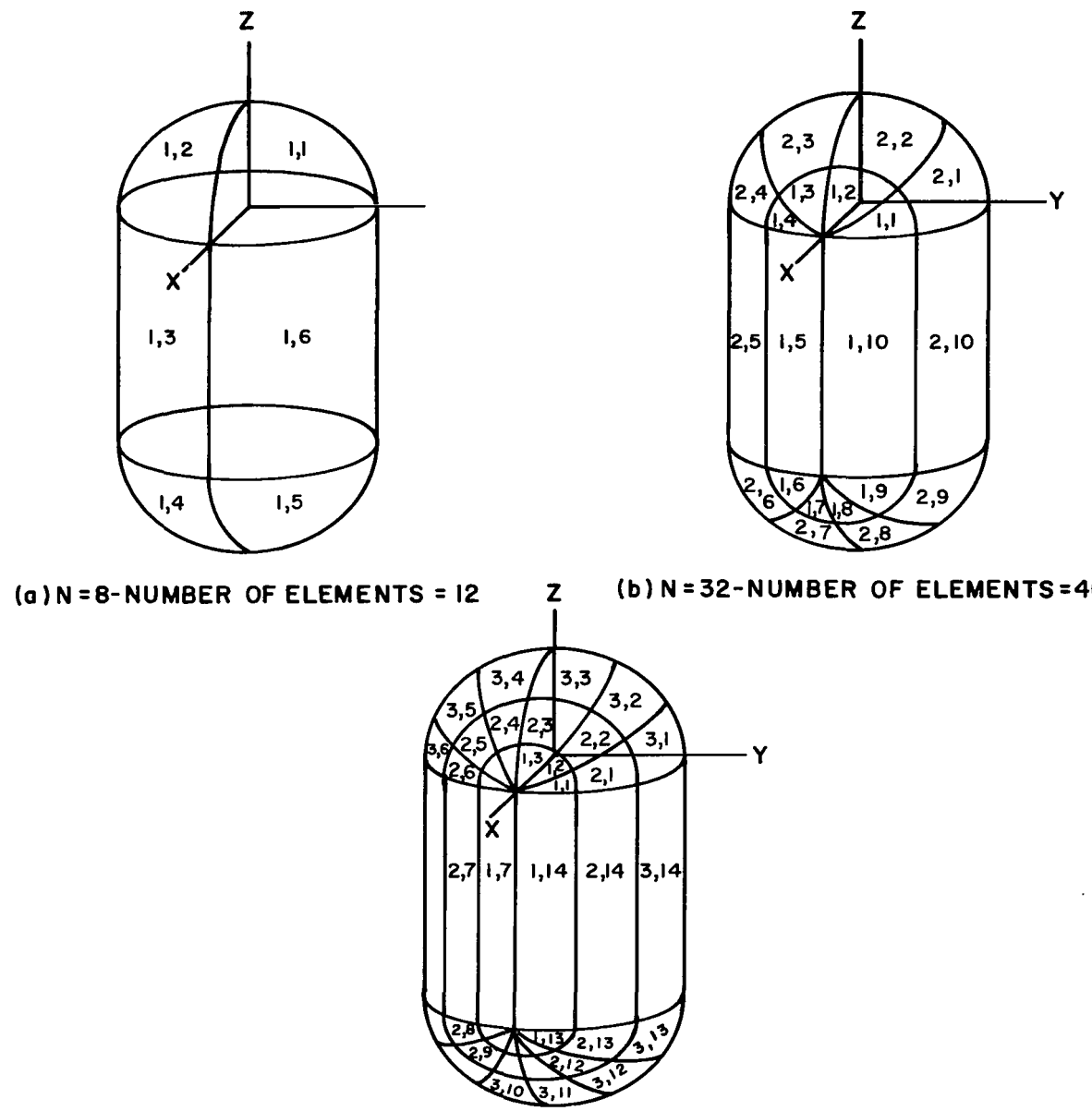

FIGURE 6. CYLINDER WITH HEMISPHERICAL ENDS (CODE NUMBER = -1)

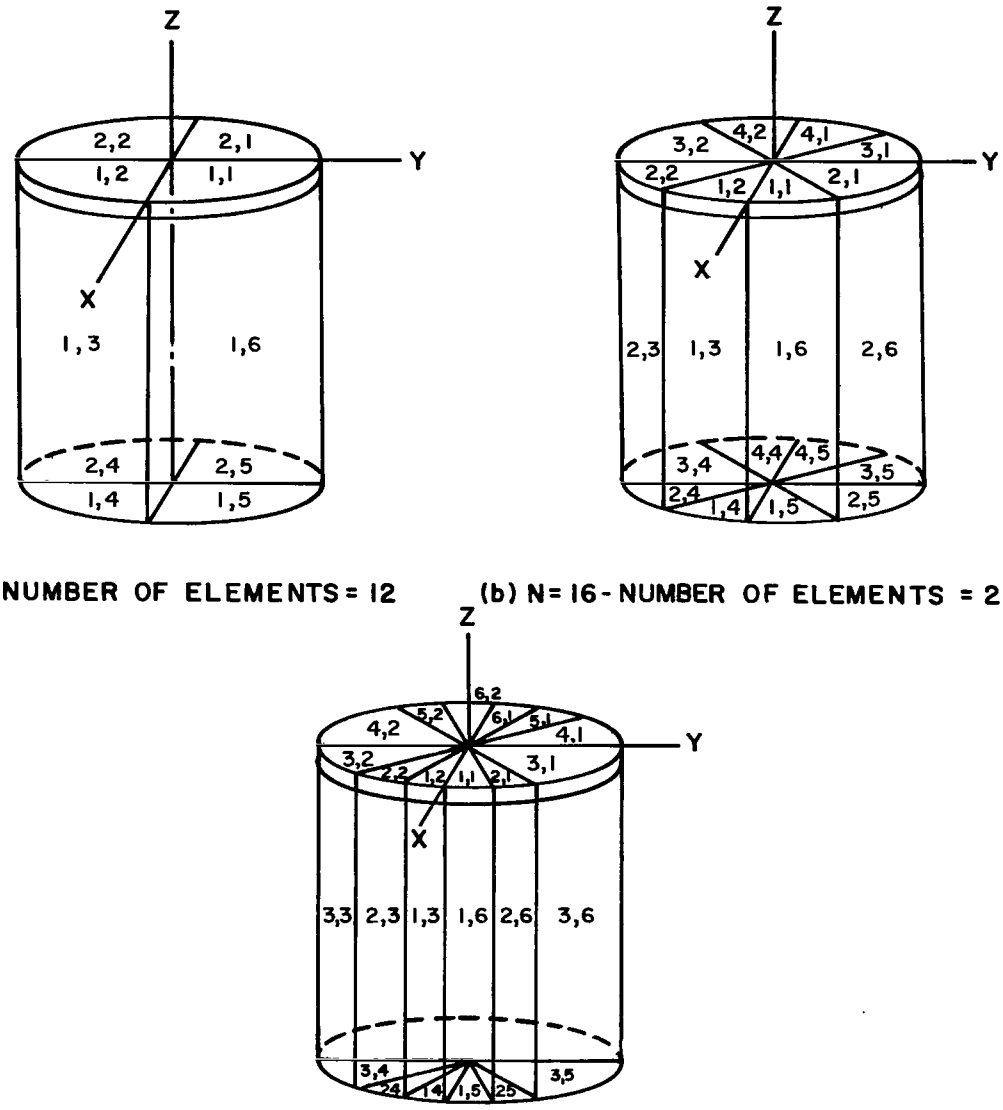

FIGURE 7. CYLINDER WITH FLAT ENDS (CODE NUMBER = +1)

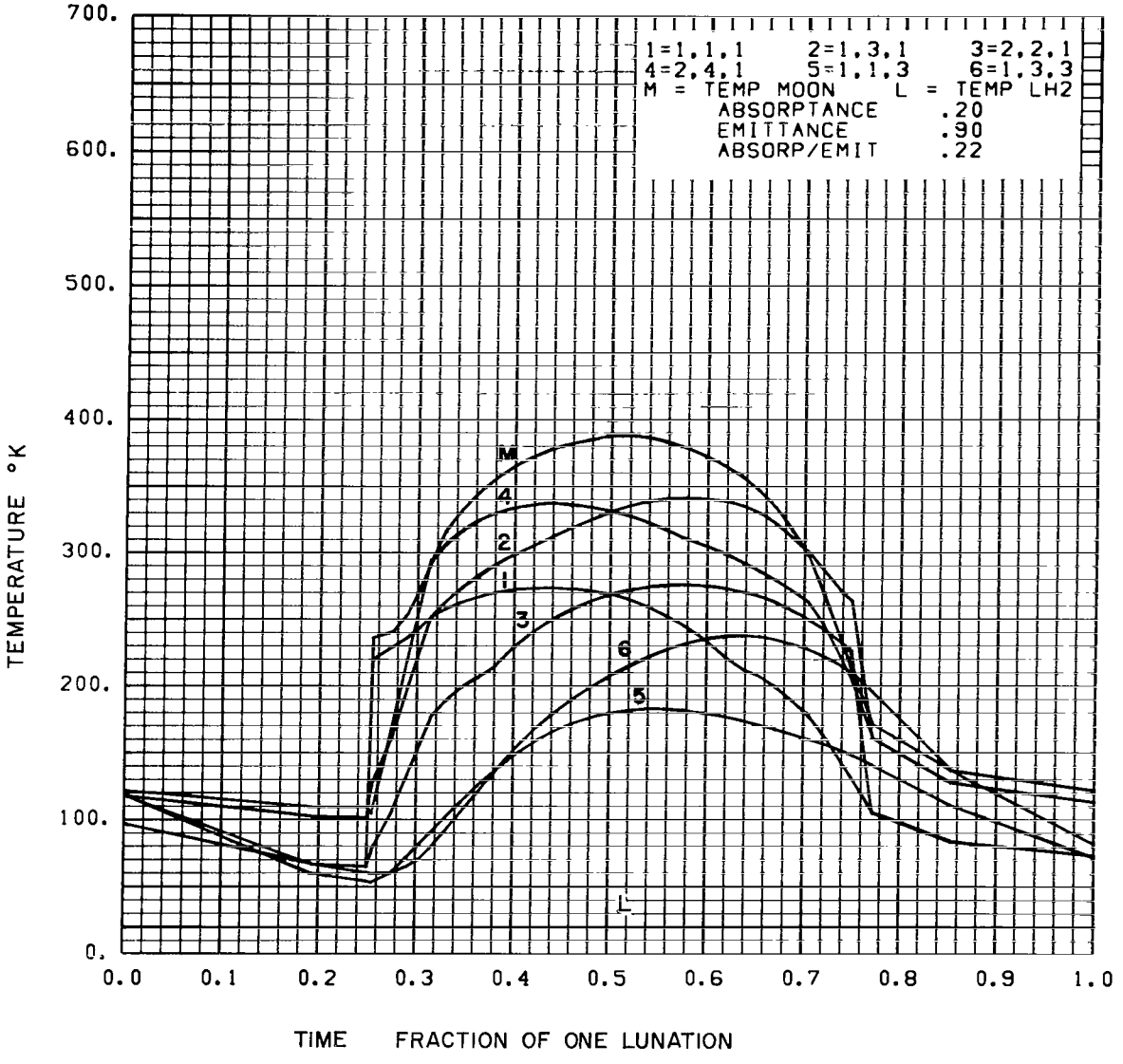

1. Zero time corresponds to the lunar midnight.
2. One lunation is equal to 708.7 hours or 29.5 earth days.
3. Element location is given in Figure 5a.

FIGURE 8. SPHERICAL TANK ELEMENT TEMPERATURE VARIATIONS (RUN 5)

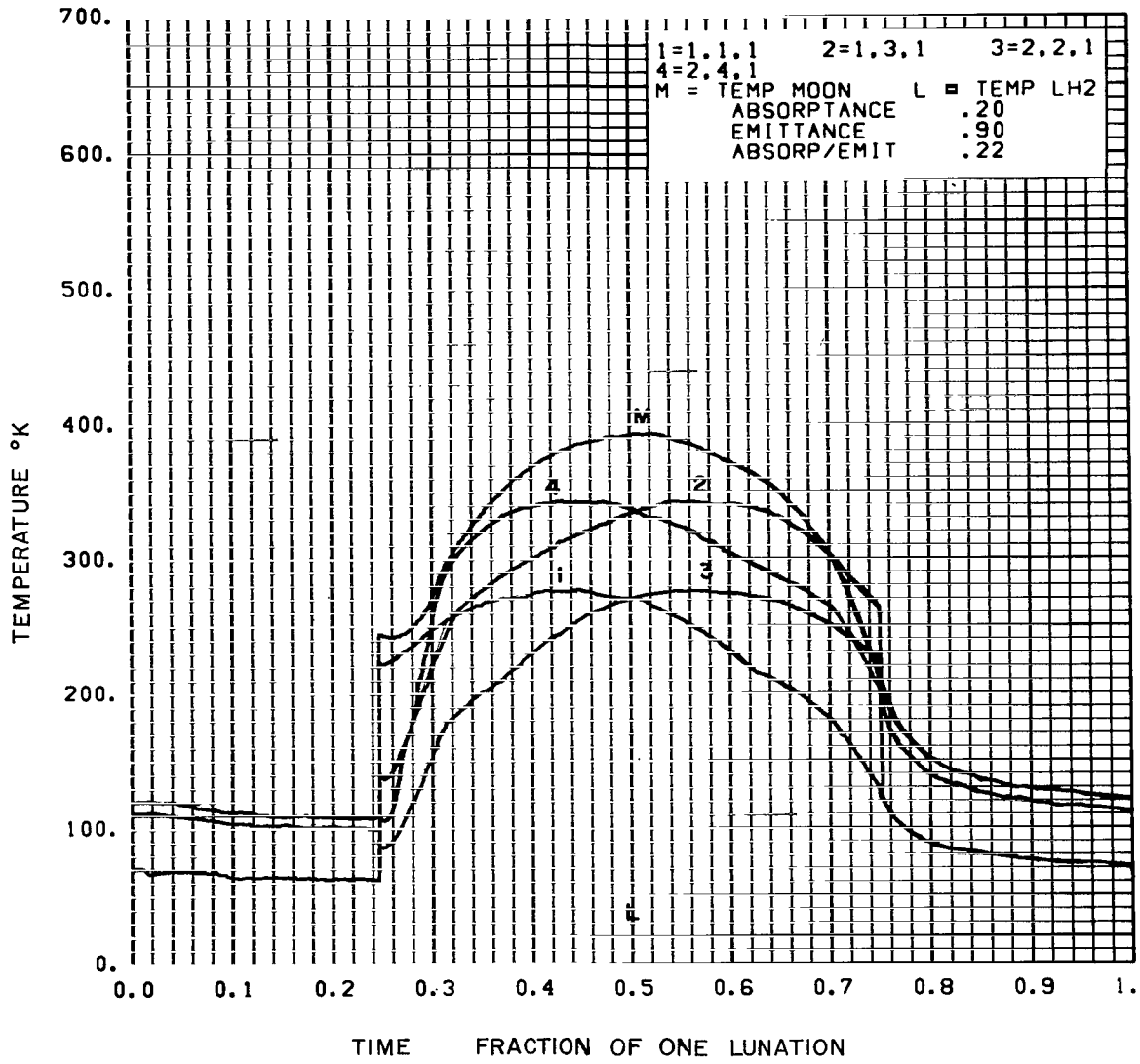

1. Zero time corresponds to the lunar midnight.
2. One lunation is equal to 708.7 hours or 29.5 earth days.
3. Element location is given in Figure 5a.

FIGURE 9. ELEMENT TEMPERATURE VARIATIONS BASED ON A THIN LAYER OF INSULATION (RUN 10)

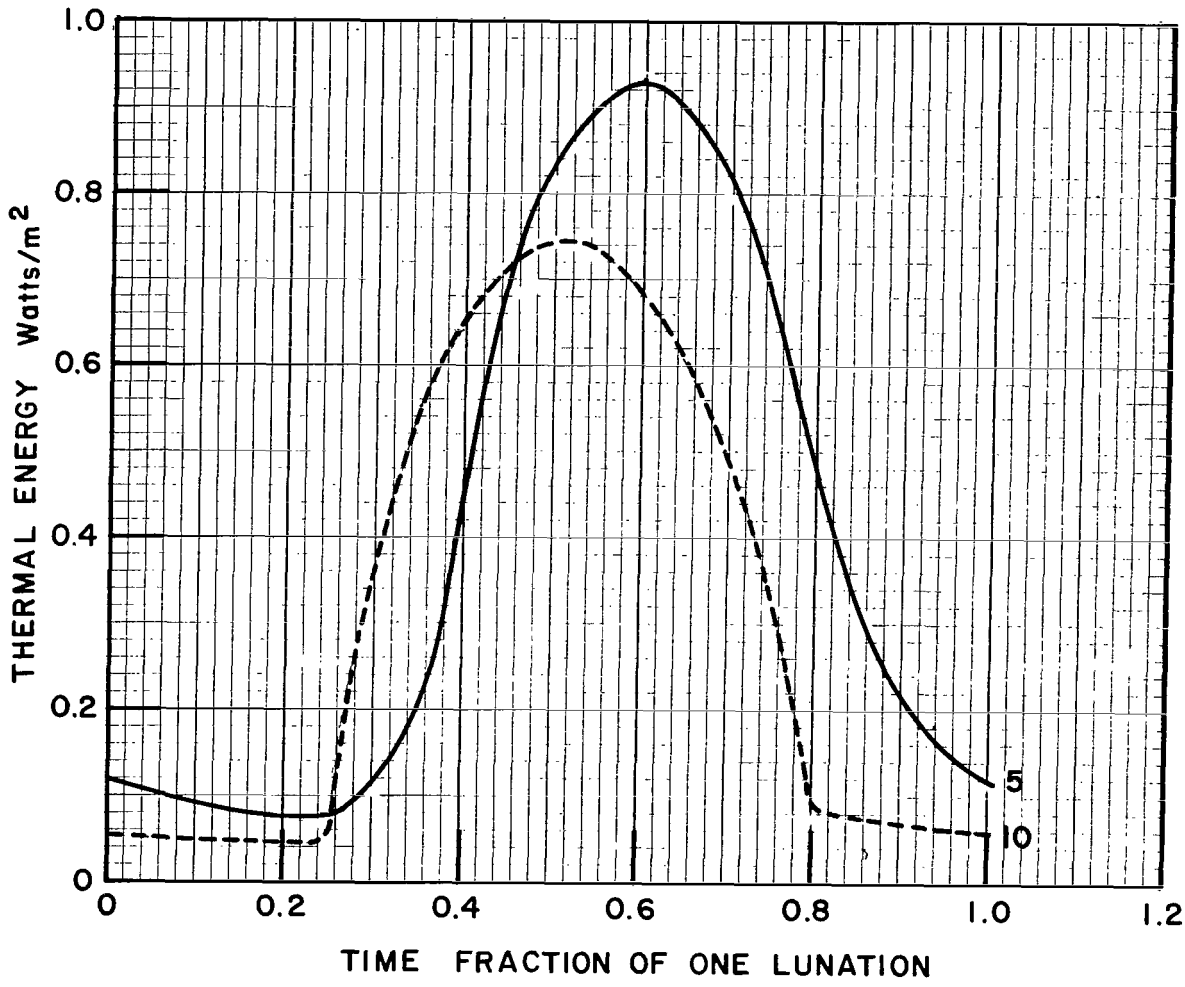

FIGURE 10. ENERGY ABSORBED BY LIQUID HYDROGEN FOR RUNS 5 AND 10

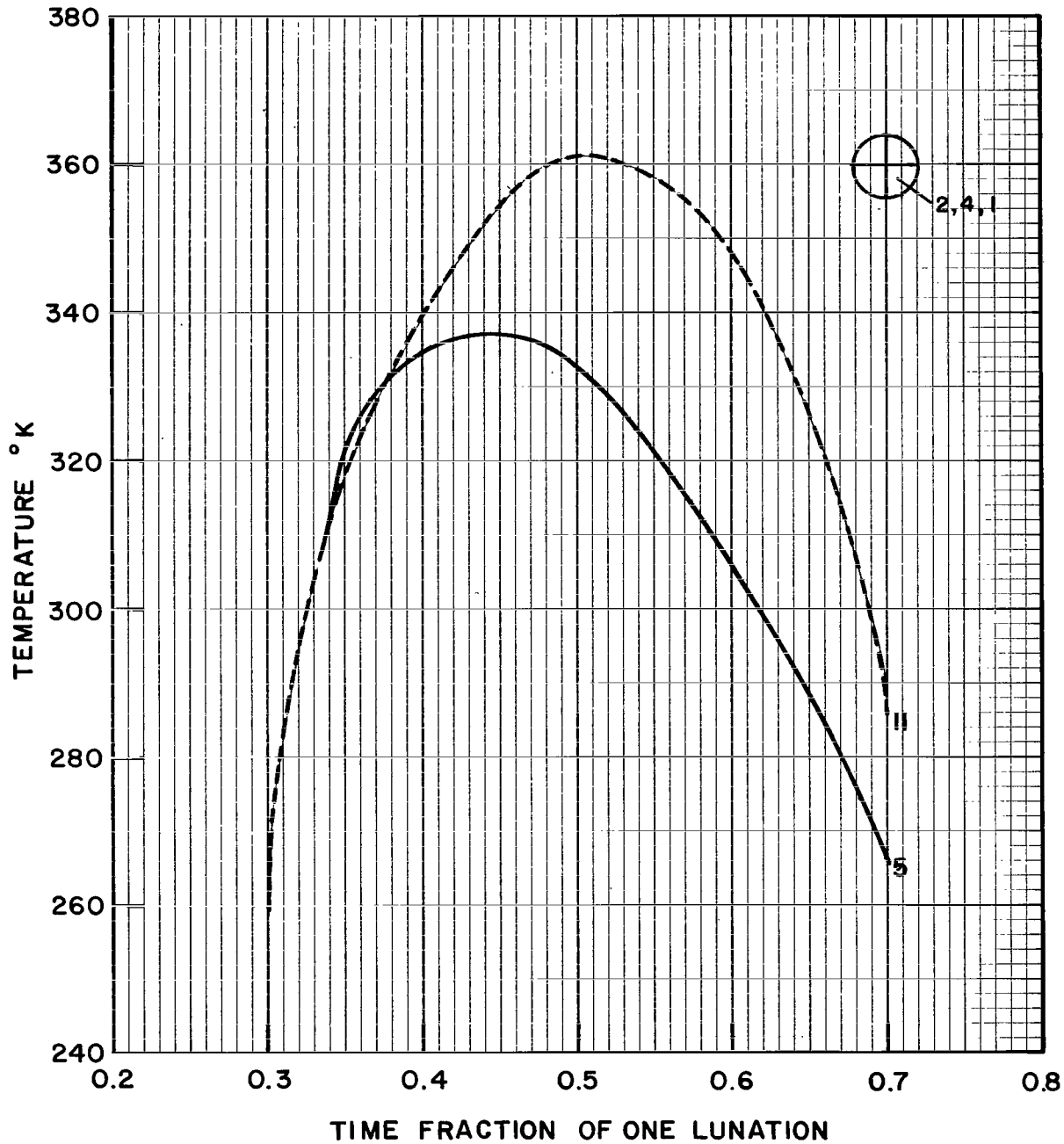

FIGURE 11. TEMPERATURE COMPARISON BETWEEN RUN 5 (SHADOW INCLUDED) AND RUN 11 (SHADOW EXCLUDED). ELEMENT 2, 4, 1

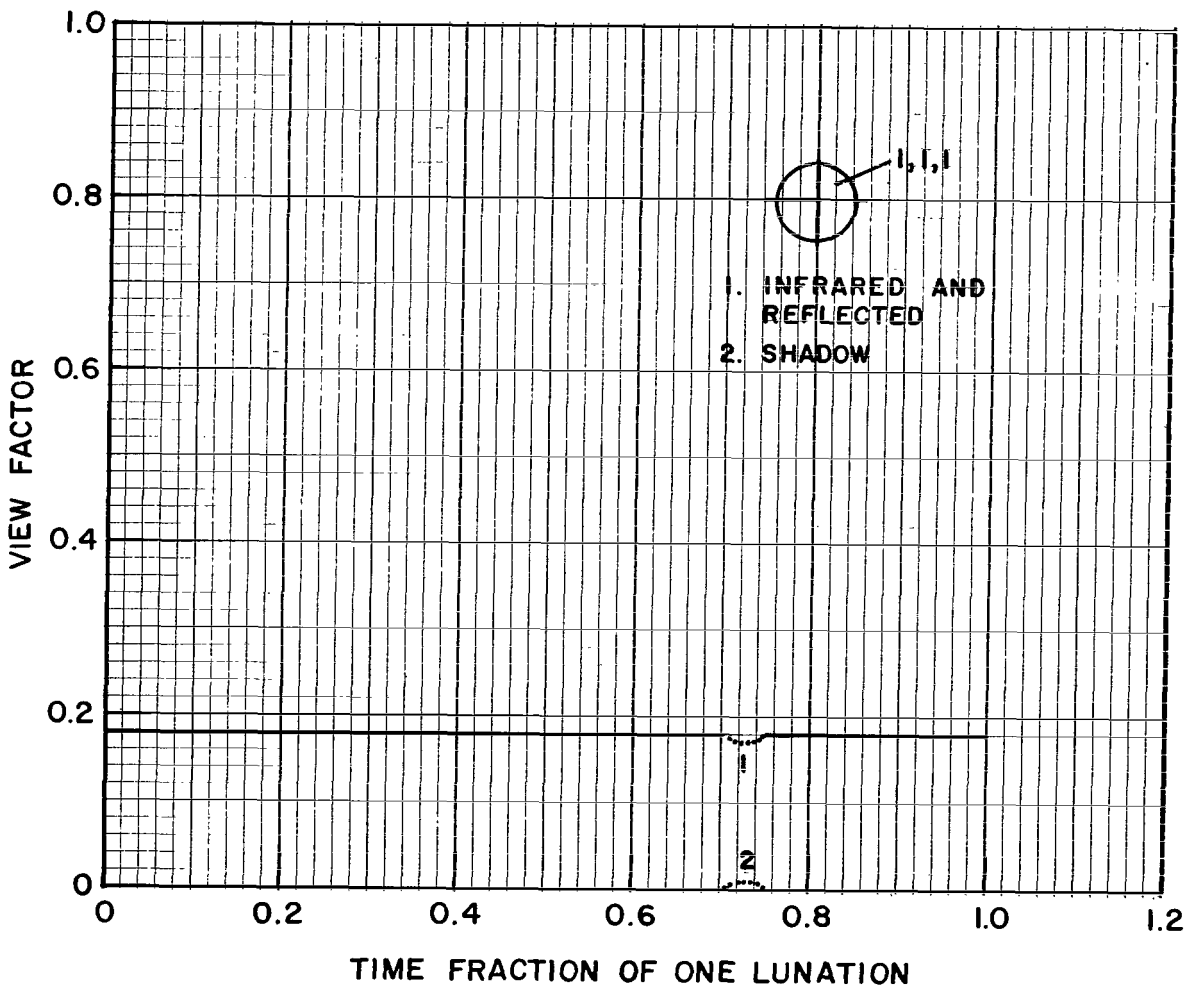

FIGURE 12. VIEW FACTORS FOR ELEMENT 1, 1, 1 (RUN 5)

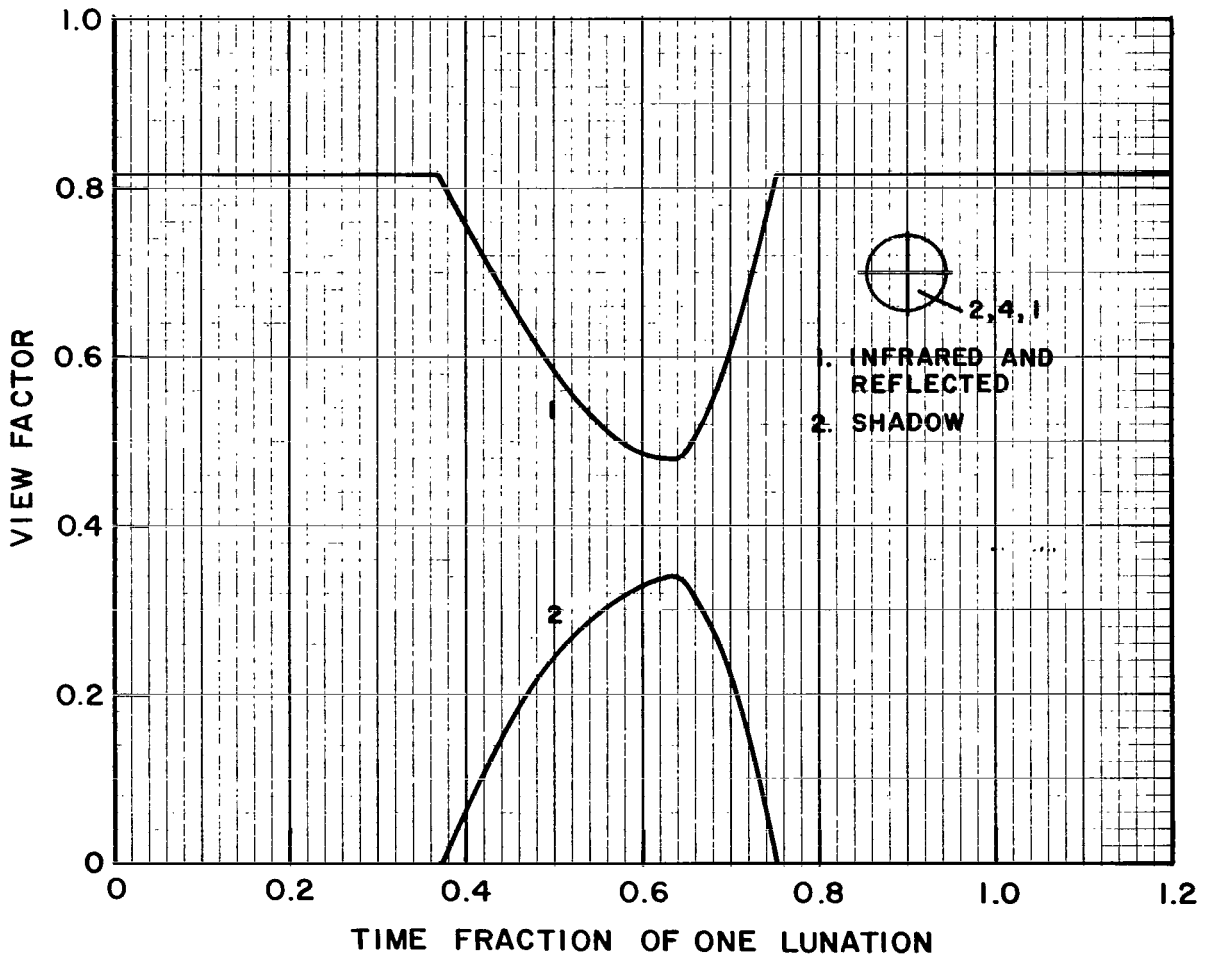

FIGURE 13. VIEW FACTORS FOR ELEMENT 2, 4, 1 (RUN 5)

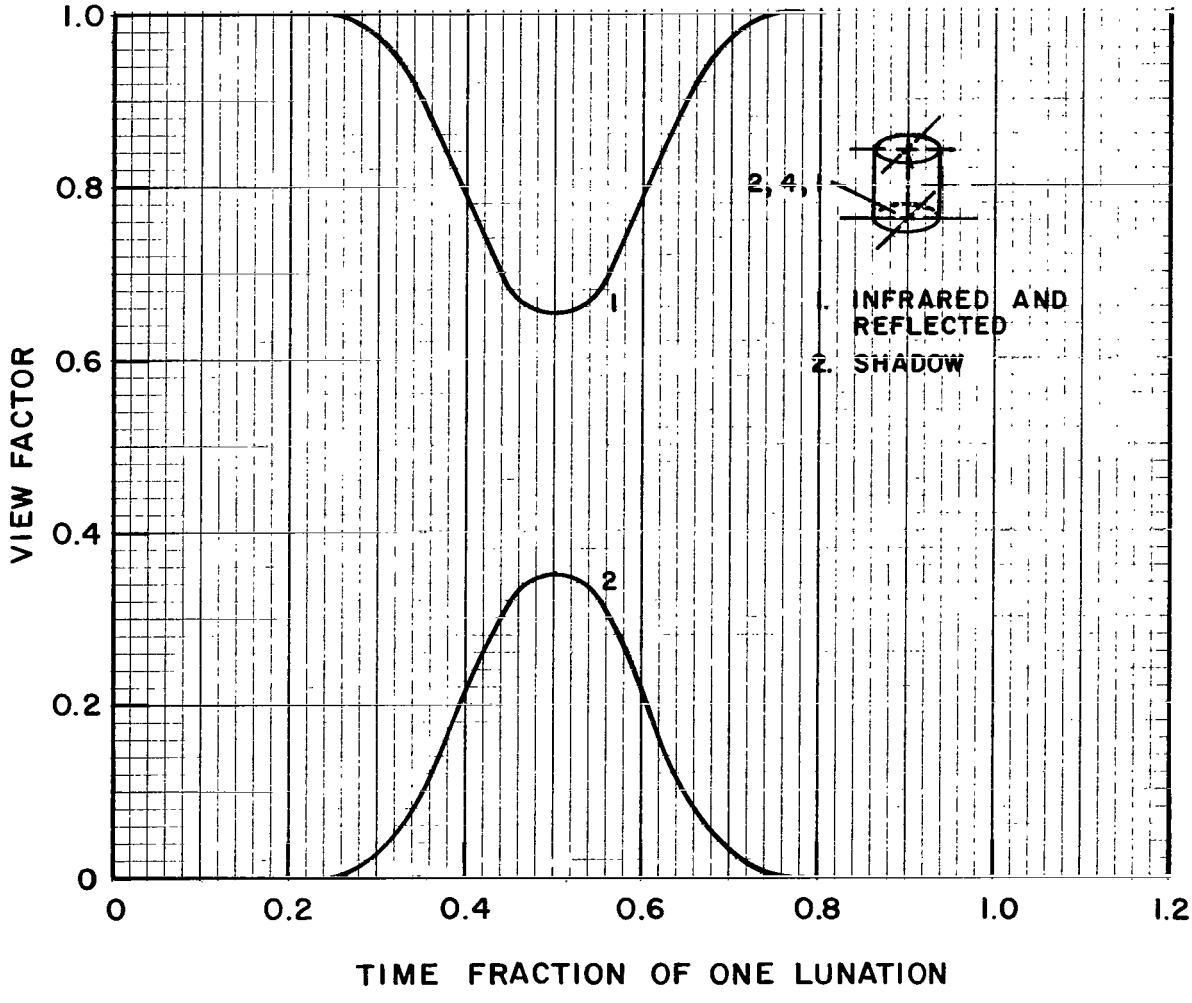

FIGURE 14. VIEW FACTORS FOR ELEMENT 2, 4, 1 (RUN 3)

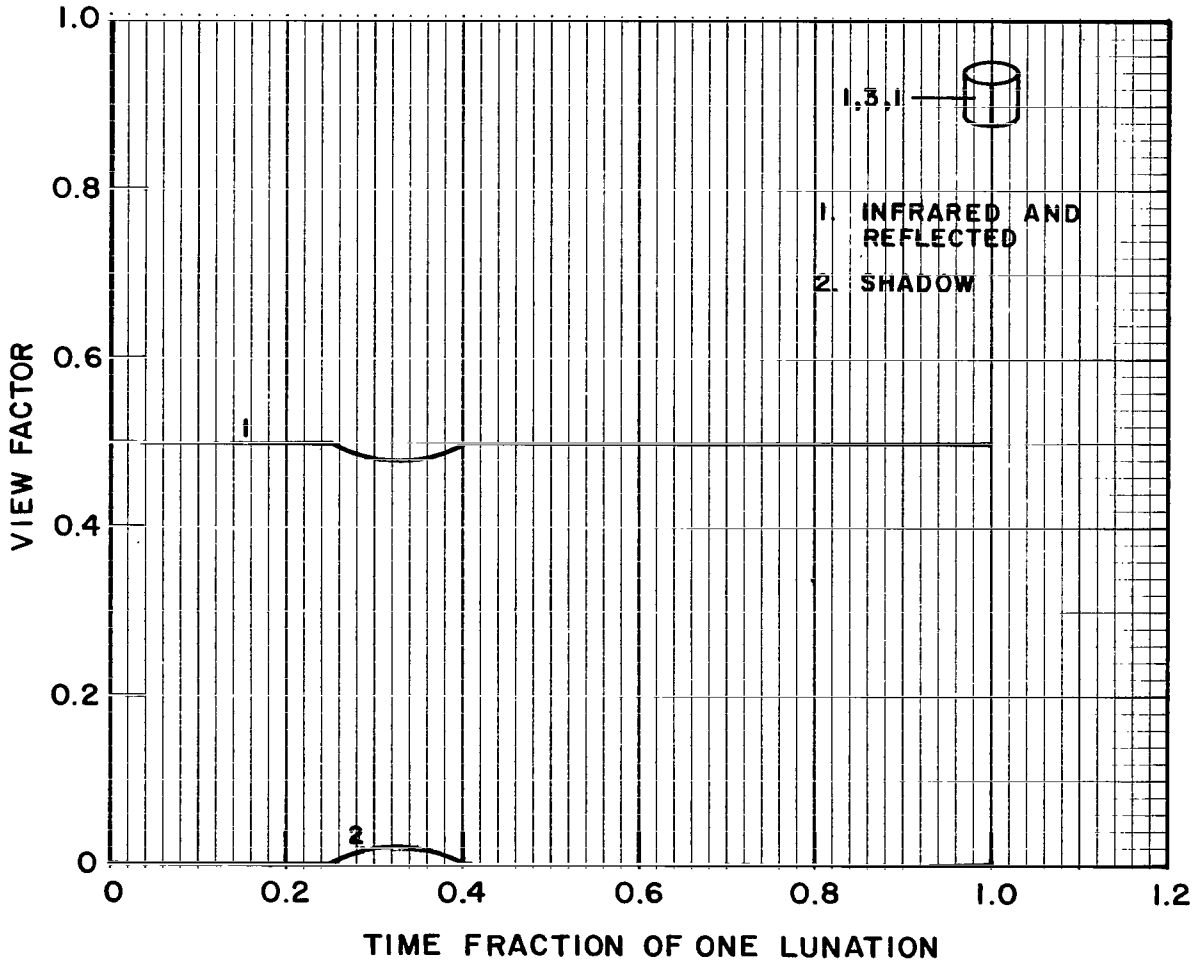

FIGURE 15. VIEW FACTORS FOR ELEMENT 1, 3, 1 (RUN 3)

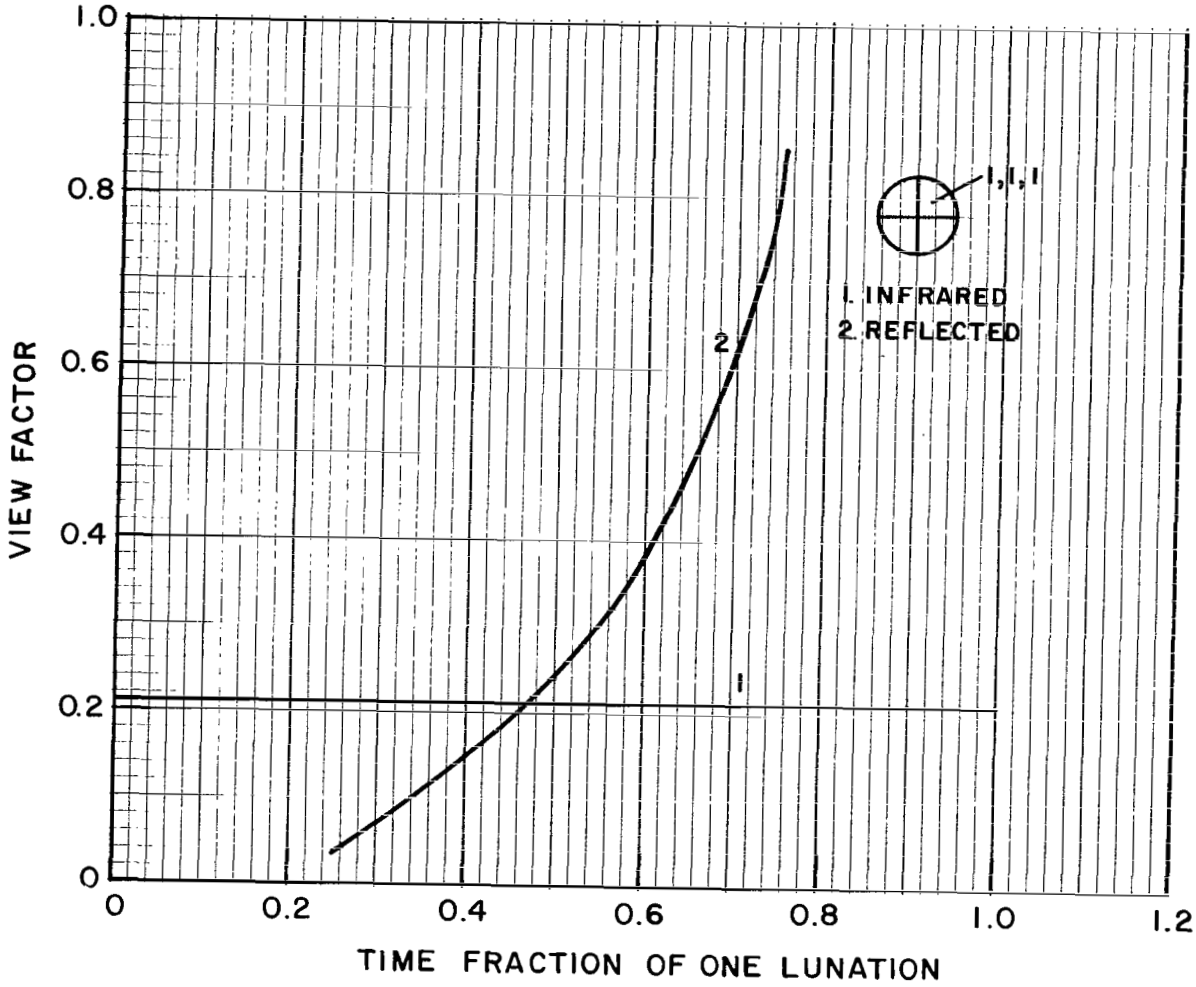

FIGURE 16. VIEW FACTORS FOR NONDIFFUSE RADIATION (RUN 20)
ELEMENT 1, 1, 1

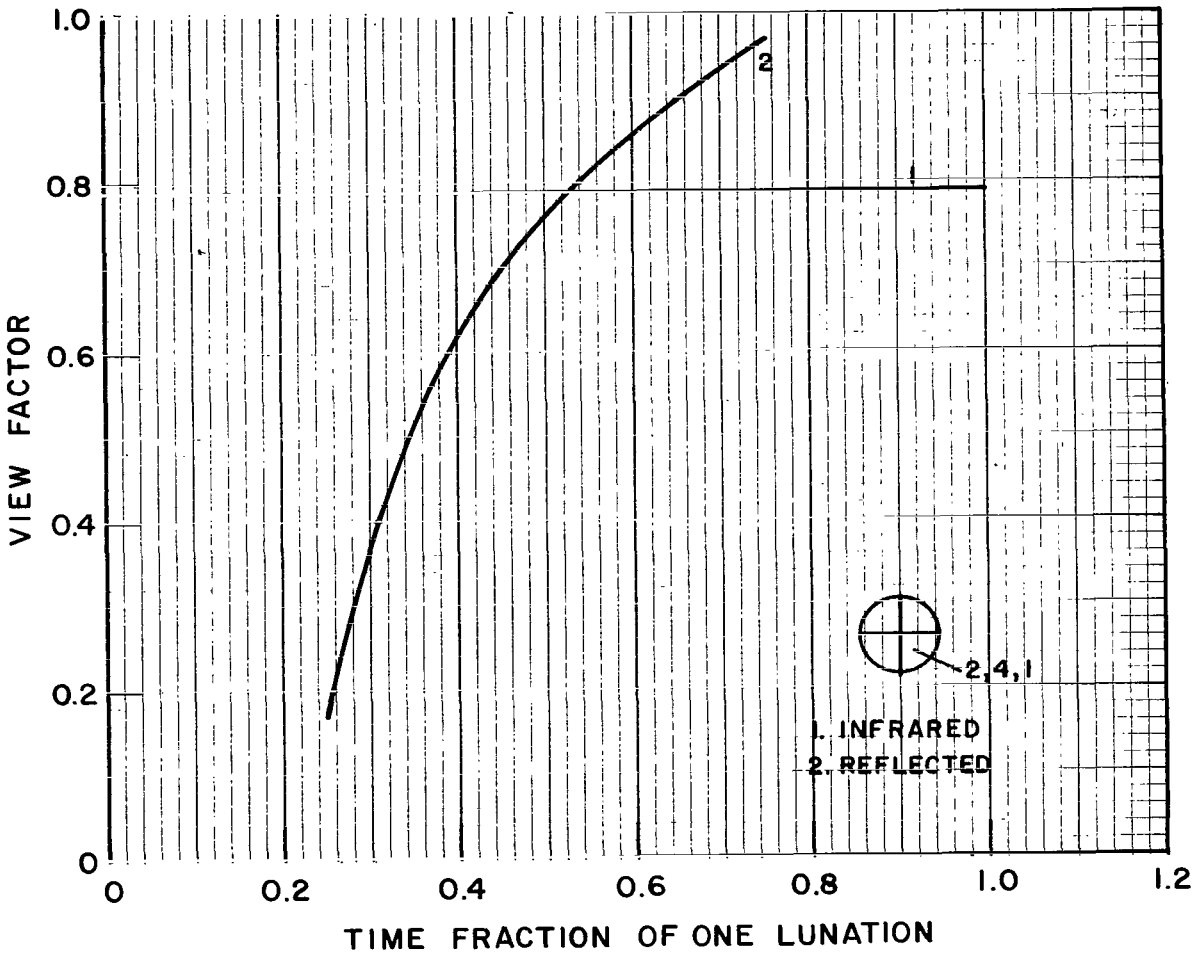

FIGURE 17. VIEW FACTORS FOR NONDIFFUSE RADIATION (RUN 20)
ELEMENT 2, 4, 1

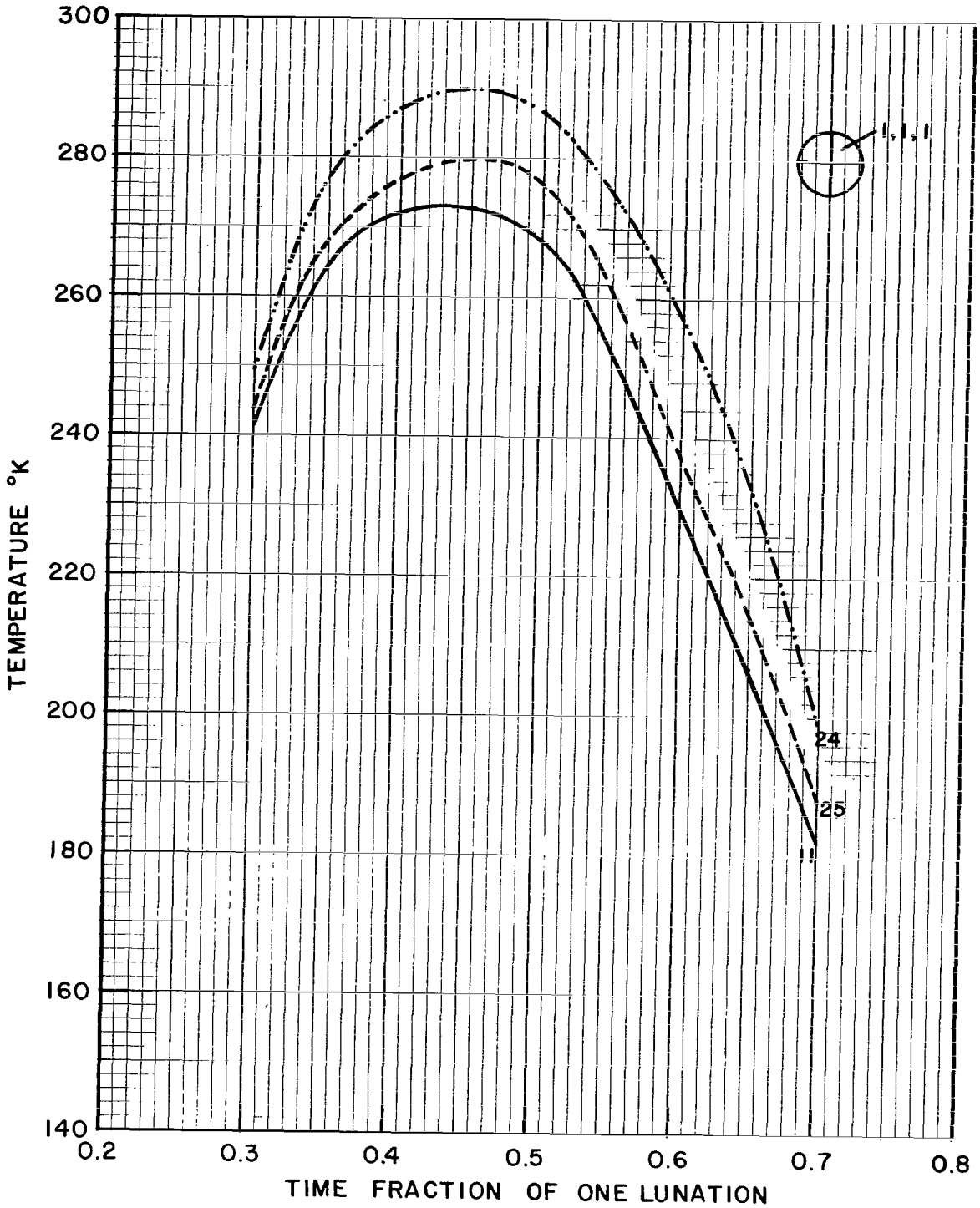

FIGURE 18. TEMPERATURE COMPARISON BETWEEN DIFFUSE COS ϵ (RUN 11), NONDIFFUSE COS $^{2/3}$ ϵ (RUN 25) AND COS$^{1/9}\epsilon$ (RUN 24) INFRARED RADIATION. ELEMENT 1, 1, 1

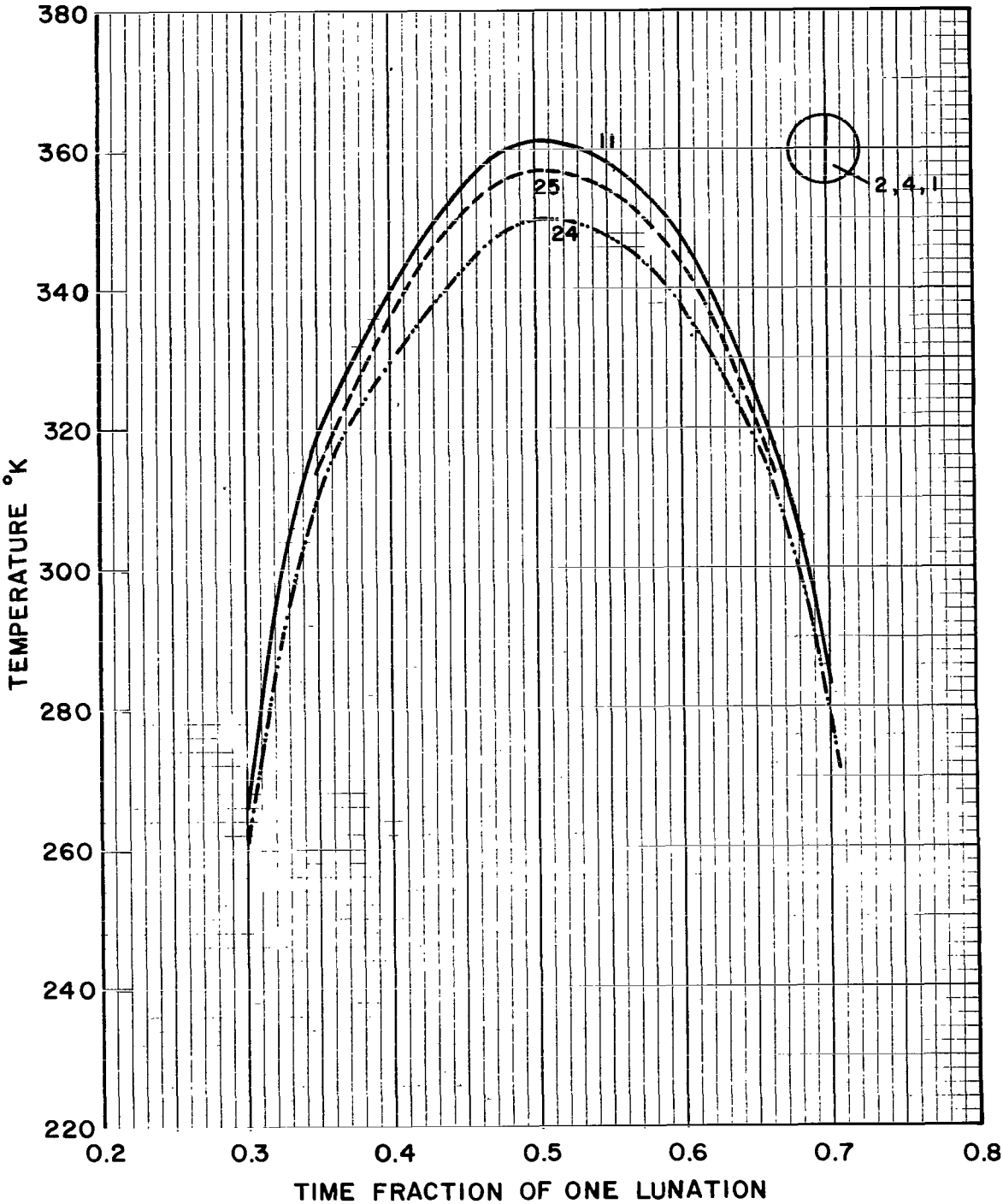

FIGURE 19. TEMPERATURE COMPARISON BETWEEN DIFFUSE COS ϵ (RUN 11), NONDIFFUSE COS $^{2/3}$ ϵ (RUN 25) AND COS $^{1/9}\epsilon$ (RUN 24) INFRARED RADIATION. ELEMENT 2, 4, 1

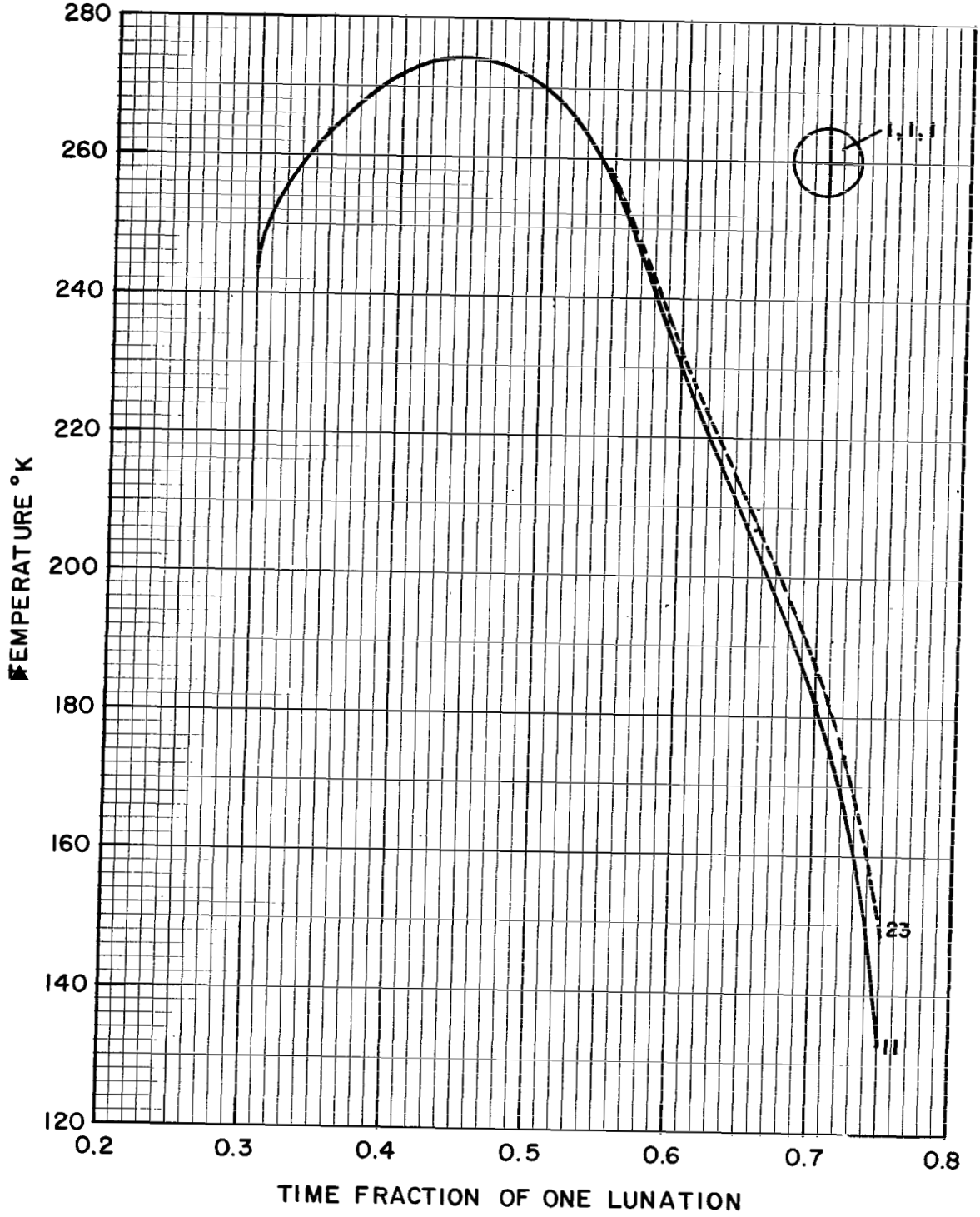

FIGURE 20. TEMPERATURE COMPARISON BETWEEN DIFFUSE (RUN 11) AND NONDIFFUSE (RUN 23) REFLECTED RADIATION. ELEMENT 1, 1, 1

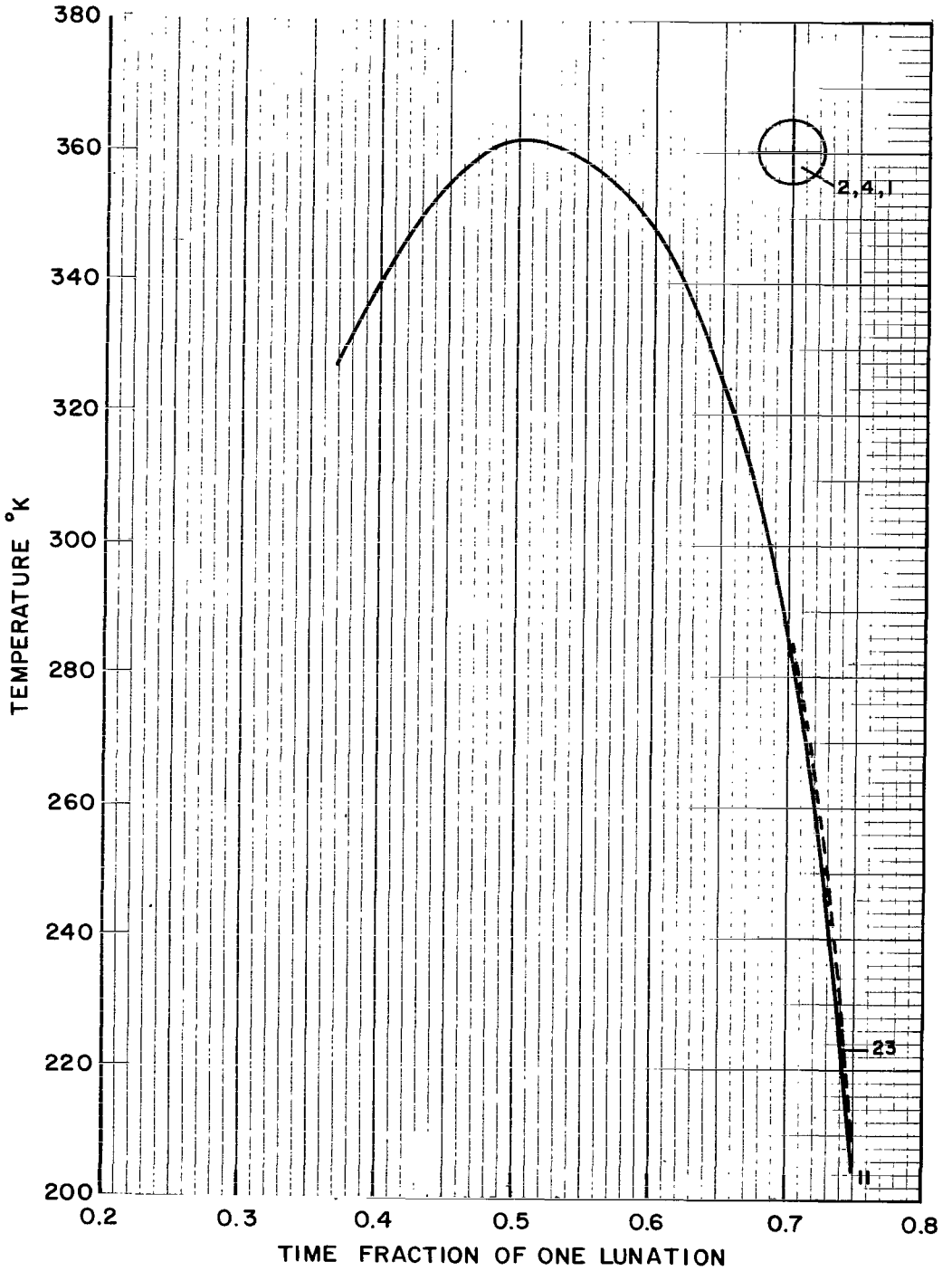

FIGURE 21. TEMPERATURE COMPARISON BETWEEN DIFFUSE (RUN 11) AND NONDIFFUSE (RUN 23) REFLECTED RADIATION. ELEMENT 2, 4, 1

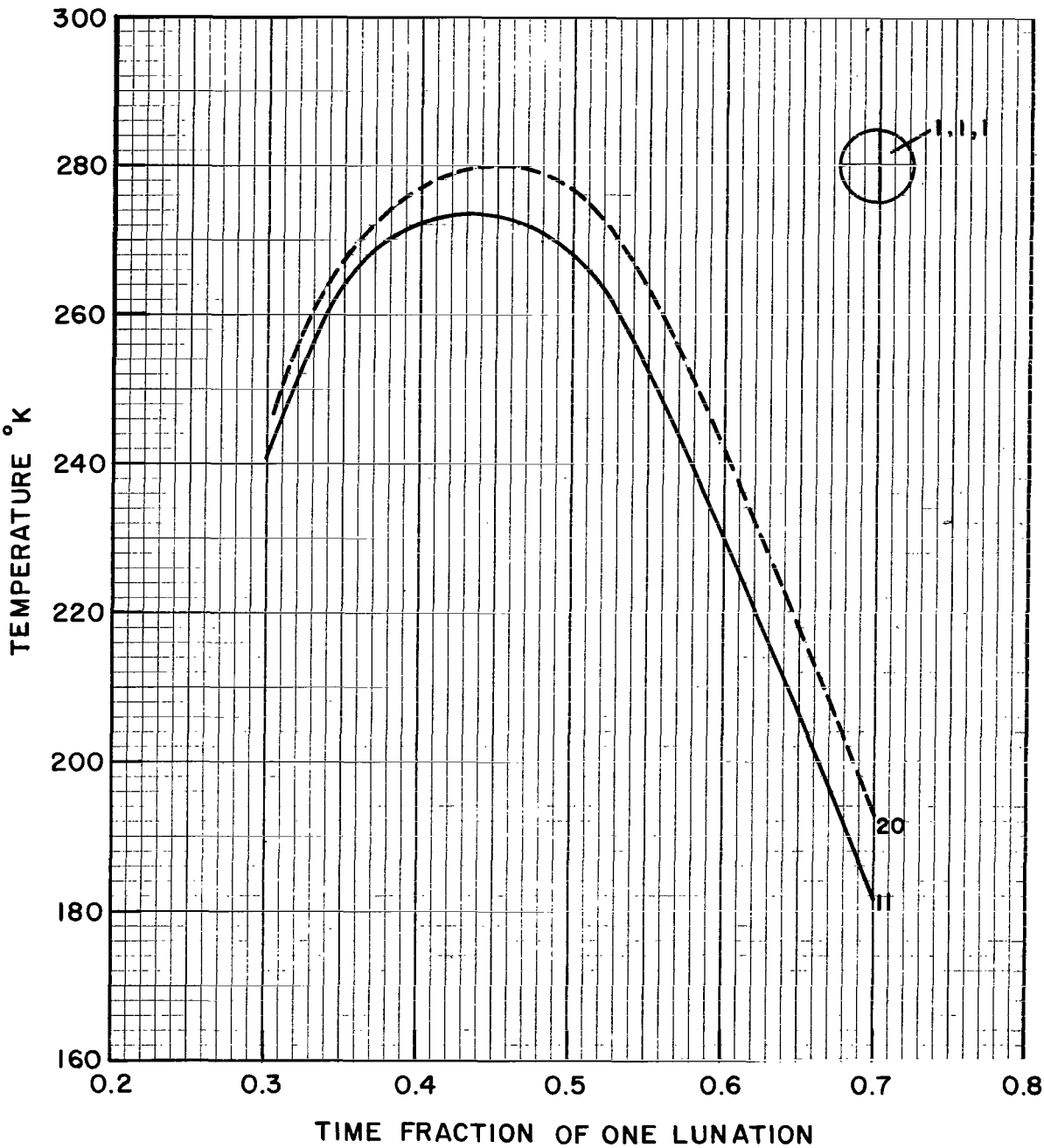

FIGURE 22. TEMPERATURE COMPARISON BETWEEN DIFFUSE (RUN 11) AND NONDIFFUSE (RUN 20) FOR COMBINED INFRARED AND REFLECTED RADIATION. ELEMENT 1, 1, 1

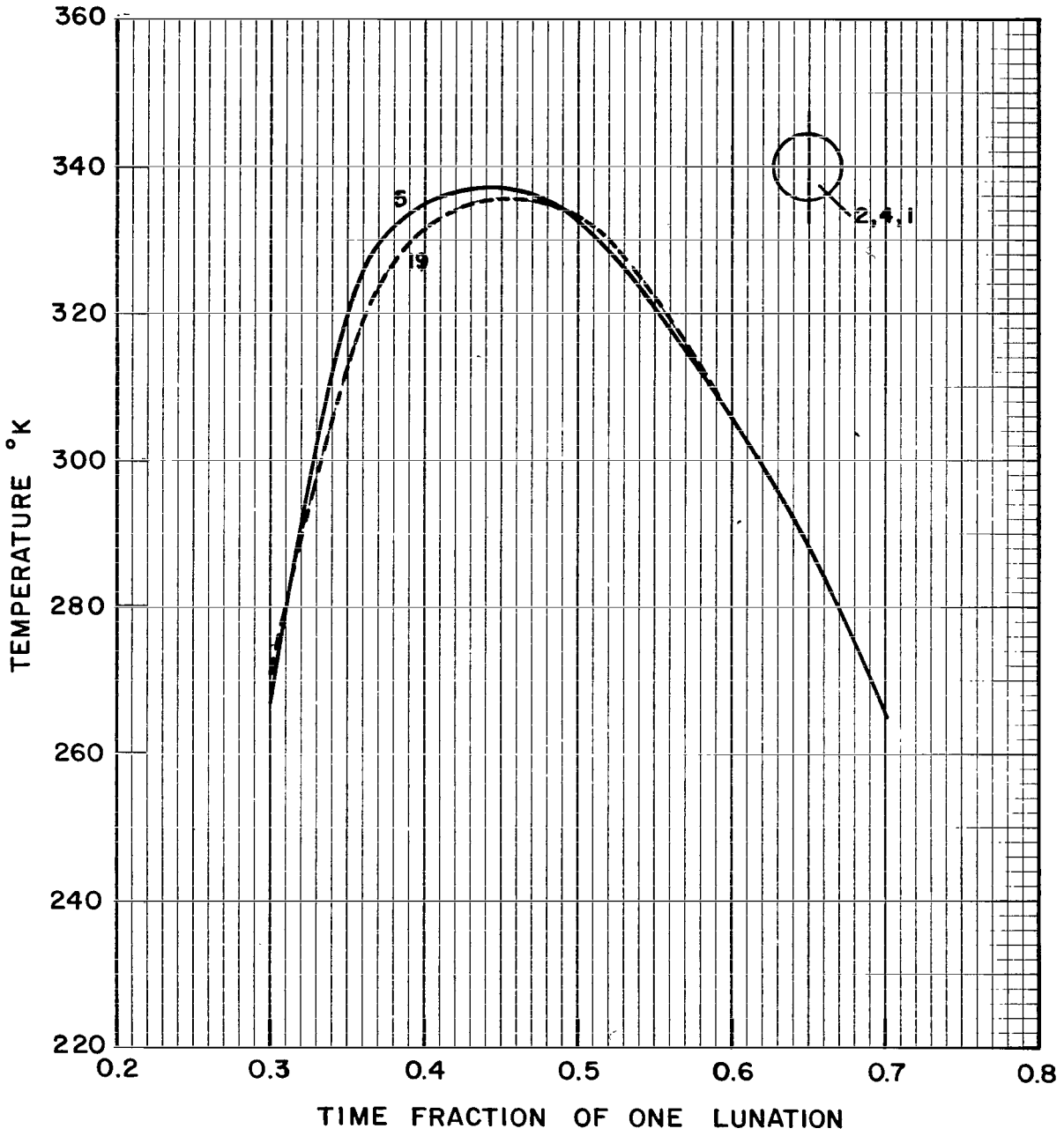

FIGURE 23. TEMPERATURE COMPARISON BETWEEN DIFFUSE (RUN 5) AND NONDIFFUSE (RUN 19) INFRARED RADIATION. ELEMENT 2, 4, 1

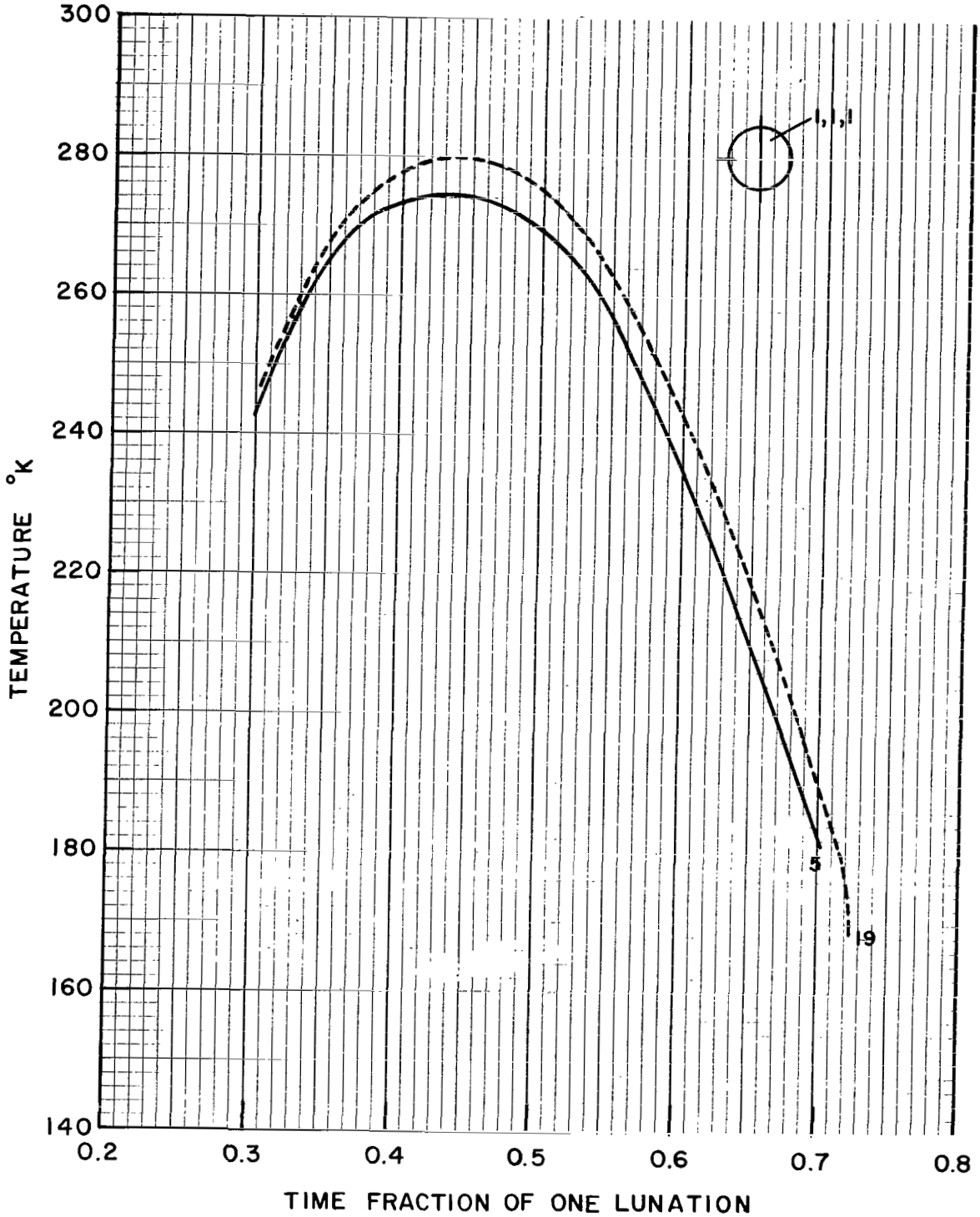

FIGURE 24. TEMPERATURE COMPARISON BETWEEN DIFFUSE (RUN 5) AND NONDIFFUSE (RUN 19) INFRARED RADIATION. ELEMENT 1, 1, 1

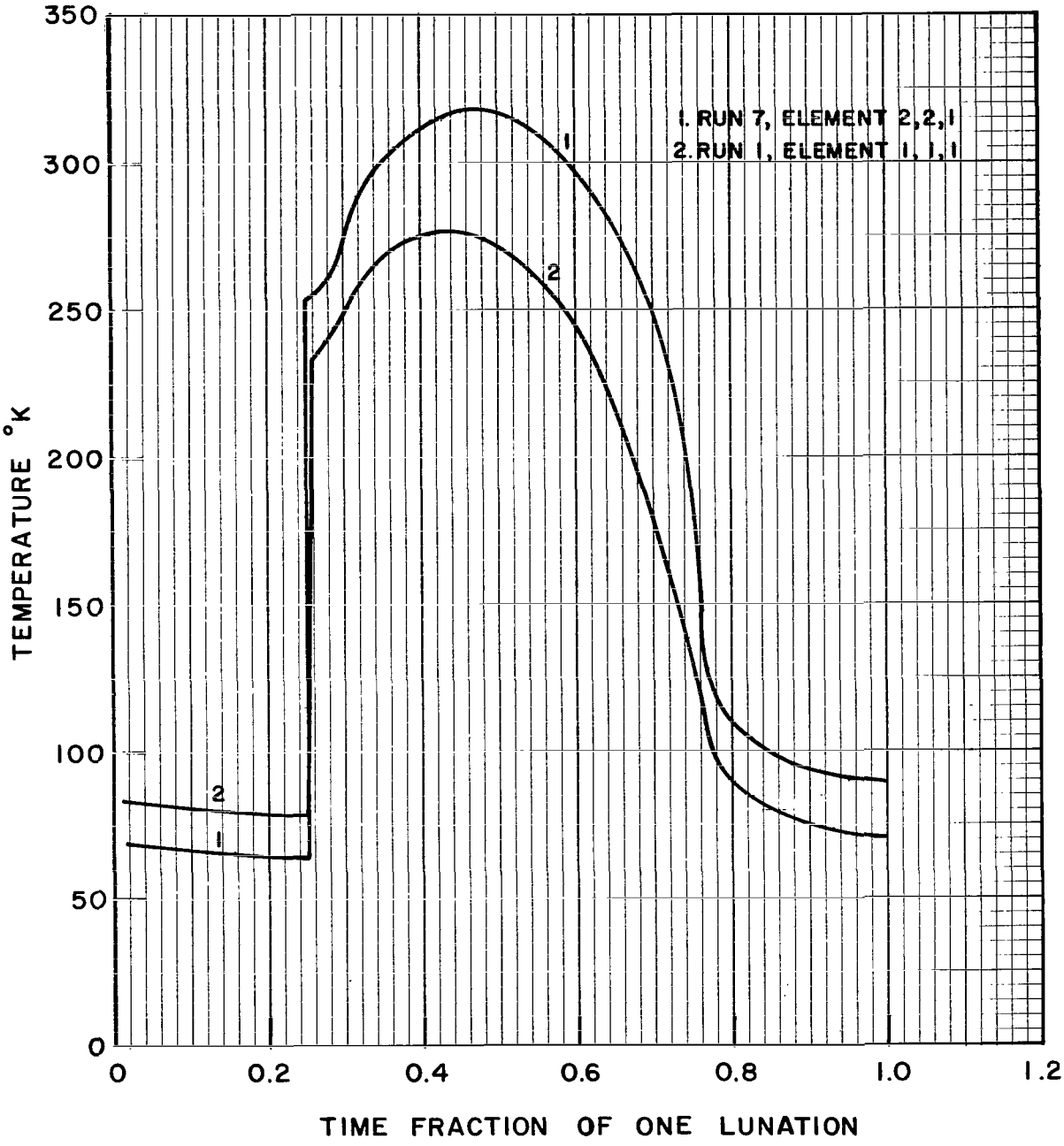

FIGURE 25. TEMPERATURE COMPARISON BETWEEN ELEMENTS OF DIFFERENT SIZE BUT SIMILAR LOCATION ON THE STORAGE VESSEL

REFERENCES

1. Anon.: Propellant Storability in Space. General Electric Co., Technical Documentary Report RPL-TDR-64-75, June 1964, p. 77.

2. Anon.: Structural and Thermal Analysis and Test of the Eight-Foot Liquid Hydrogen Tank. Boeing Co., Document No. D2-23278, May 11, 1965, pp. 114 and 127.

3. Dempster, W. E.; Evans, R. L.; and Olivier, J. R.: Lunar Storage of Liquid Propellants. NASA TN D-1117, July 1962.

4. Pettit, E.; and Nicholson, S. B.: Astrophys. J., 1930, pp. 71-102.

5. Hapke, Bruce W.: A Theoretical Photometric Function for the Lunar Surface. J. Geophys. Res., vol. 68, 1963, pp. 4571-4586.

6. Harrison, J. K.; and Hilliard, J. W.: Computer Program - Cryogenic Storage on the Moon (Subroutines A and C). NASA TM X-53270, June 9, 1965.

7. Russell, L. D.: A Parametric Study of the Lunar Thermal Diffusivity Employing a Fourier Series. NASA-MSFC, M-RP-INT-63-11, 1963.

8. Kopal, Zdenek: Physics and Astronomy of the Moon. Academic Press, Ch. 11, 1962.

9. Little, Arthur D., Inc.: Study of Cryogenic Storage on the Moon. Final Report on Contract NAS8-11377, December 1965.

10. Todd, John: Survey of Numerical Analysis. McGraw-Hill Book Co., Inc., 1962, p. 319.

11. Jones, B. P.: A Study of Several Numerical Methods for Solving a Particular System of Ordinary Differential Equations. NASA TM X-53121, Aug.5, 1964.

12. Blackwell, J.: Cryogenic Storage on the Moon, Documentation Job No. 346414, Computation Laboratory, Marshall Space Flight Center, Aug. 1966.

13. Scott, R. B.: Cryogenic Engineering, D. Van Nostrand Company, Inc., Ch. 9, 1959.

14. Timmerhaus, K. D., ed.: Advances in Cryogenic Engineering, Engineering Aspects of Heat Transfer in Multilayer Reflective Insulation, and Performance of NRC Insulation. vol. 5, Plenum Press, 1959, p. 199.

15. Anon.: Handbook of Chemistry and Physics. 43 ed., Chemical Rubber Publishing Co., 1961, p. 1452.

16. Mikesell, R. P; and Scott, R. B.: Heat Conduction through Insulating Supports in Very Low Temperature Equipment. J. Res. N.B.S., vol. 57, no. 6, Research Paper 2726, Dec. 1956.

17. Timmerhaus, K. D., ed.: Advances in Cryogenic Engineering, Thermal Analysis and Optimization of Cryogenic Tanks for Lunar Storage, vol. 11, 1965.

NASA-Langley, 1967 M420

"The aeronautical and space activities of the United States shall be conducted so as to contribute . . . to the expansion of human knowledge of phenomena in the atmosphere and space. The Administration shall provide for the widest practicable and appropriate dissemination of information concerning its activities and the results thereof."

—NATIONAL AERONAUTICS AND SPACE ACT OF 1958

NASA SCIENTIFIC AND TECHNICAL PUBLICATIONS

TECHNICAL REPORTS: Scientific and technical information considered important, complete, and a lasting contribution to existing knowledge.

TECHNICAL NOTES: Information less broad in scope but nevertheless of importance as a contribution to existing knowledge.

TECHNICAL MEMORANDUMS: Information receiving limited distribution because of preliminary data, security classification, or other reasons.

CONTRACTOR REPORTS: Technical information generated in connection with a NASA contract or grant and released under NASA auspices.

TECHNICAL TRANSLATIONS: Information published in a foreign language considered to merit NASA distribution in English.

TECHNICAL REPRINTS: Information derived from NASA activities and initially published in the form of journal articles.

SPECIAL PUBLICATIONS: Information derived from or of value to NASA activities but not necessarily reporting the results of individual NASA-programmed scientific efforts. Publications include conference proceedings, monographs, data compilations, handbooks, sourcebooks, and special bibliographies.

Details on the availability of these publications may be obtained from:

SCIENTIFIC AND TECHNICAL INFORMATION DIVISION

NATIONAL AERONAUTICS AND SPACE ADMINISTRATION

Washington, D.C. 20546